Spinons in Spatially Anisotropic Frustrated Antiferromagnets

June 8th, 2007

Masanori Kohno

Physics department, UCSB
NIMS, Japan

Collaborators: Leon Balents (UCSB)
& Oleg Starykh (Univ. Utah)

Outline

- **Introduction**

  Elementary excitations in antiferromagnets : Magnon & Spinon
  Experimental indications of 2D spin liquids

- **Model & Method**

  Spatially anisotropic frustrated antiferromagnetic Heisenberg model
  Weak interchain-coupling approach

- **Results**

  Momentum-dependent spectral features
  Bound State of Spinons ~ Triplon ~

- **Comparison with Experiments**

  Dynamical Structure Factor observed in Cs_2CuCl_4

Elementary Excitations in Antiferromagnets

Excitation	Magnon	Spinon
Physical	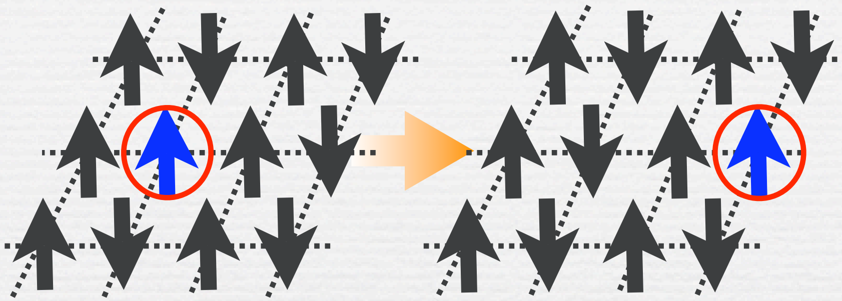	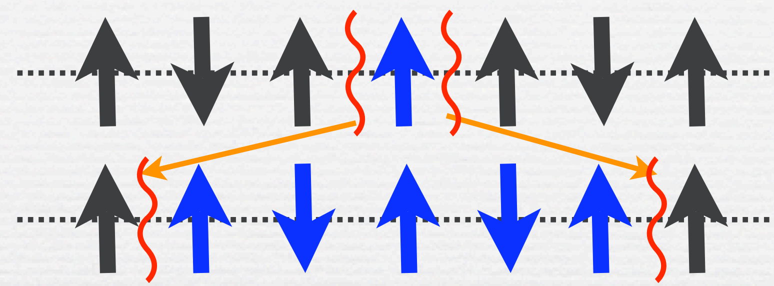
Spin	1	1/2
G.S.	Long-range order	Spin-singlet
		
Systems	Unfrustrated in D >1	1D

Elementary Excitations in Antiferromagnets

Excitation	Magnon	Spinon
Physical	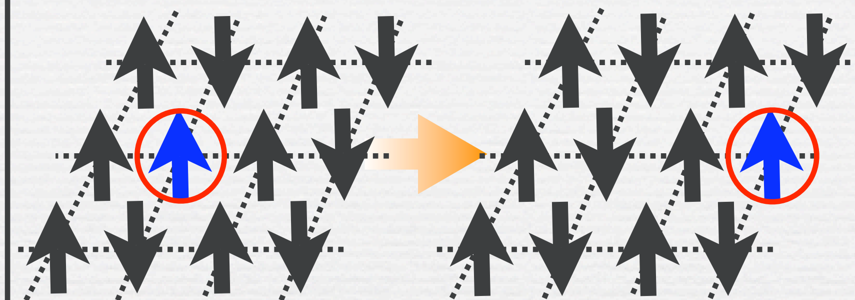	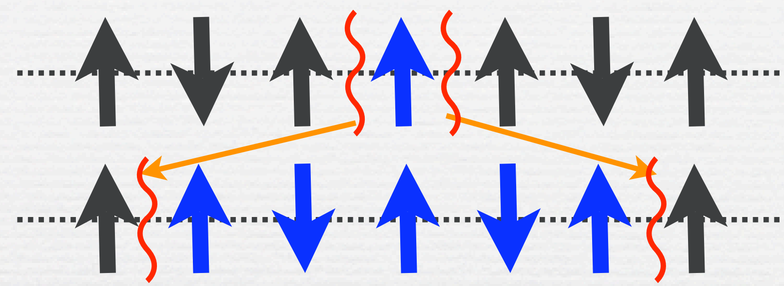
Spin	1	1/2
G.S.	Long-range order	Spin-singlet
		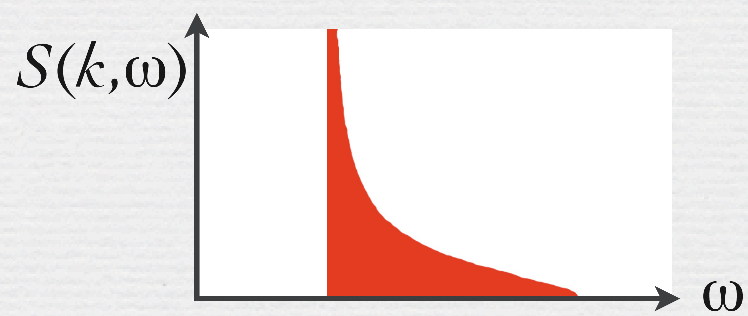
Systems	Unfrustrated in D >1	1D

Highly frustrated antiferromagnets in D>1?

Experimental Indications of 2D Spin liquids

- Ground state without long-range order:

  · Triangular lattice: κ-(BETT-TTF)$_2$Cu$_2$(CN)$_3$
  Solid ^{3}He in 2D

  · Kagome lattice : ZnCu$_3$(OH)$_6$Cl$_2$

… No signature of long-range order down to T<<J [ex. T~32 mK, J~250 K]

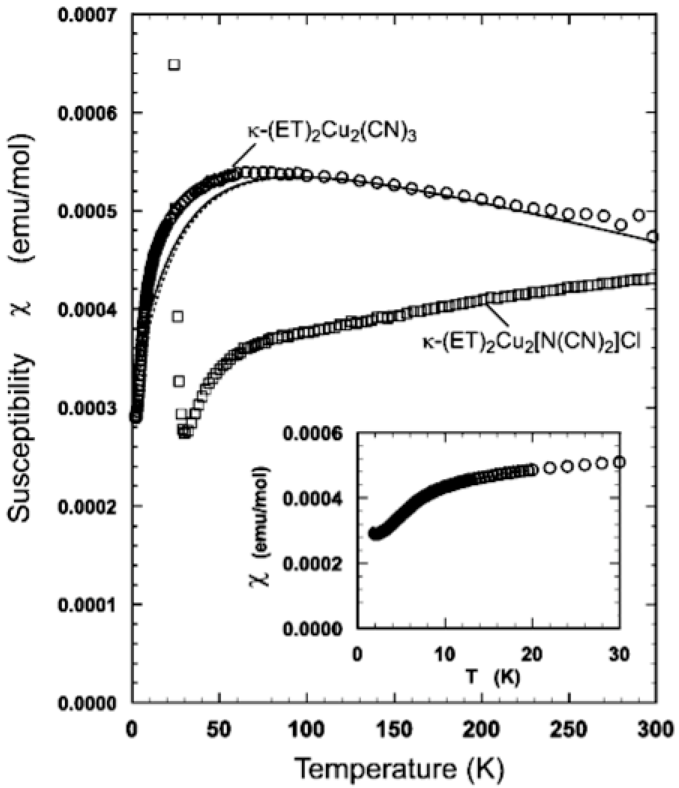

Y.Shimizu *et al*, PRL **91** , 107001 (2003).

Experimental Indications of 2D Spin liquids

- Ground state without long-range order:

 · Triangular lattice: κ-(BETT-TTF)$_2$Cu$_2$(CN)$_3$

 Solid ^{3}He in 2D

 · Kagome lattice : ZnCu$_3$(OH)$_6$Cl$_2$

... No signature of long-range order down to T<<J [ex. T~32 mK, J~250 K]

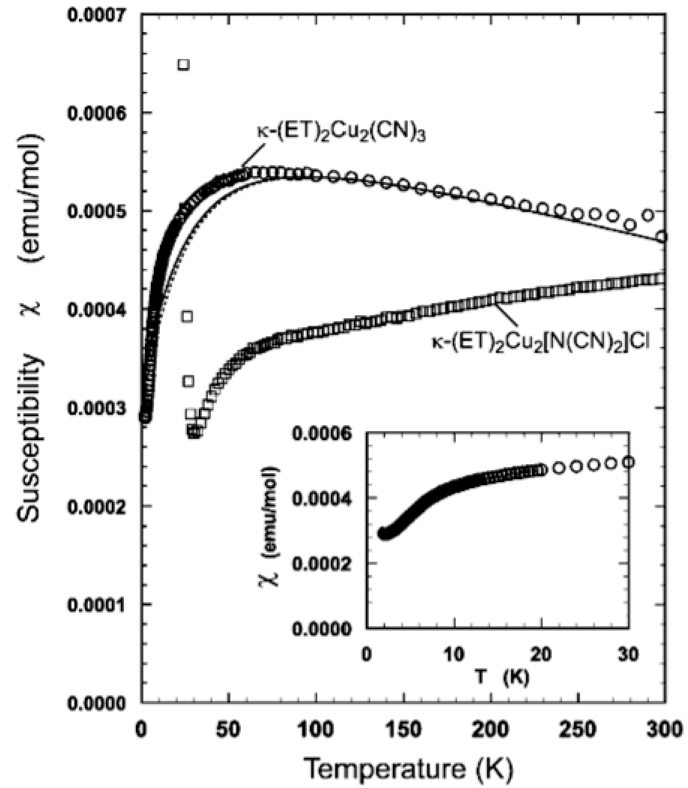

Y.Shimizu *et al*, PRL **91** , 107001 (2003).

- Non-magnon excitation:

 · Triangular lattice with spatial anisotropy : Cs$_2$CuCl$_4$

Experimental Indications of 2D Spin liquids

- Ground state without long-range order:

  · Triangular lattice: κ-(BETT-TTF)$_2$Cu$_2$(CN)$_3$

  Solid ^{3}He in 2D

  · Kagome lattice : ZnCu$_3$(OH)$_6$Cl$_2$

  … No signature of long-range order down to T<<J [ex. T~32 mK, J~250 K]

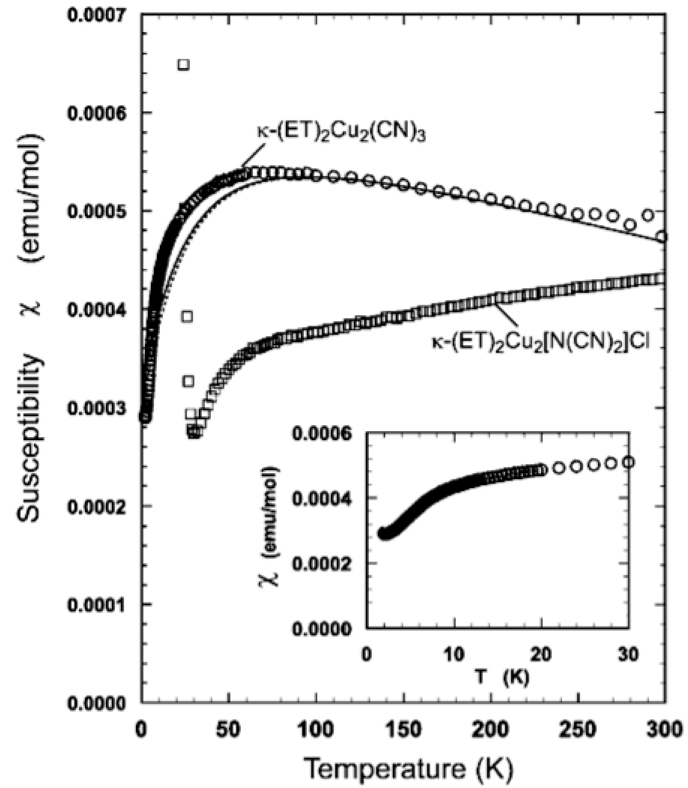

Y.Shimizu *et al*, PRL **91** , 107001 (2003).

- Non-magnon excitation:

  · Triangular lattice with spatial anisotropy : Cs$_2$CuCl$_4$

Large Tail of $S(k,\omega)$ in Cs_2CuCl_4

Line shape in Cs_2CuCl_4

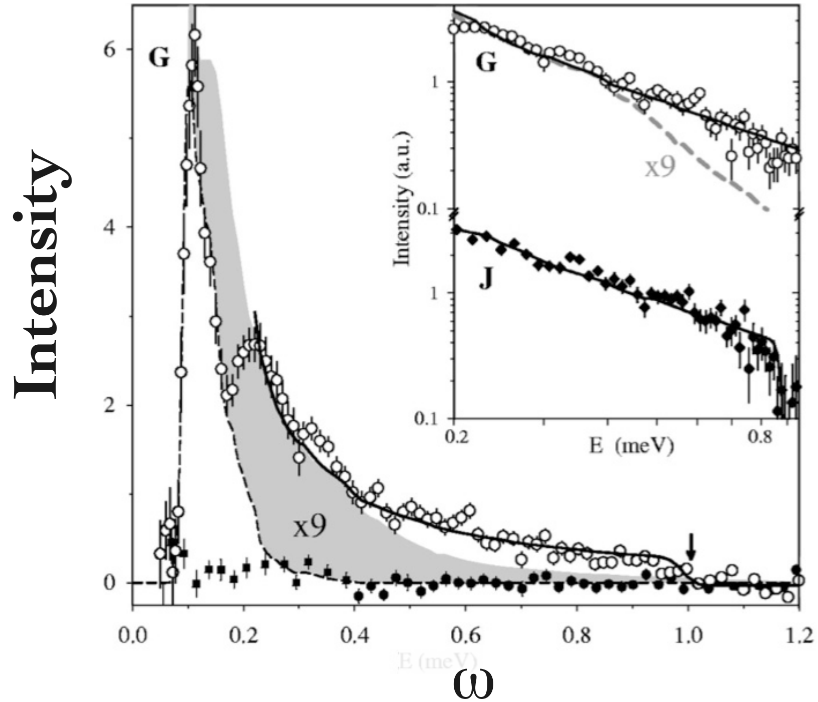

Dynamical structure factor $S(k, \omega)$ at $k_x=\pi$[1]

Spinon :

Power-law divergence with a large tail.

Magnon :

δ-functional peak with negligible tail.

[1] R.Coldea, *et al.*, Phys. Rev. B **68**, 134424 (2003).

Typical Magnon
(for comparison)

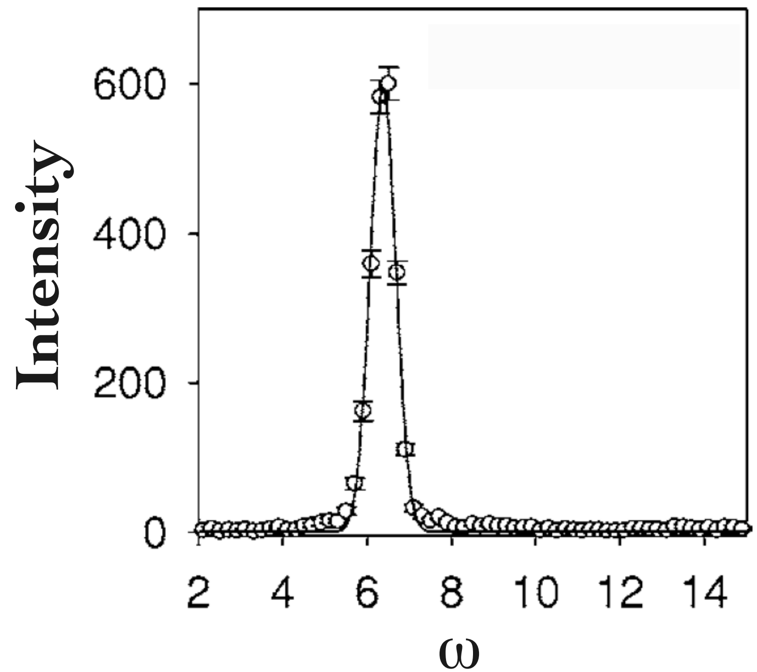

Line shape in Rb_2MnF_4

[square lattice, S=5/2 at $\boldsymbol{k}$=(π,0.3π)]

T.Huberman, *et al.*,
Phys. Rev. B. **72** 014413 (2005).

Large Tail of $S(k,\omega)$ in Cs_2CuCl_4

Line shape in Cs_2CuCl_4

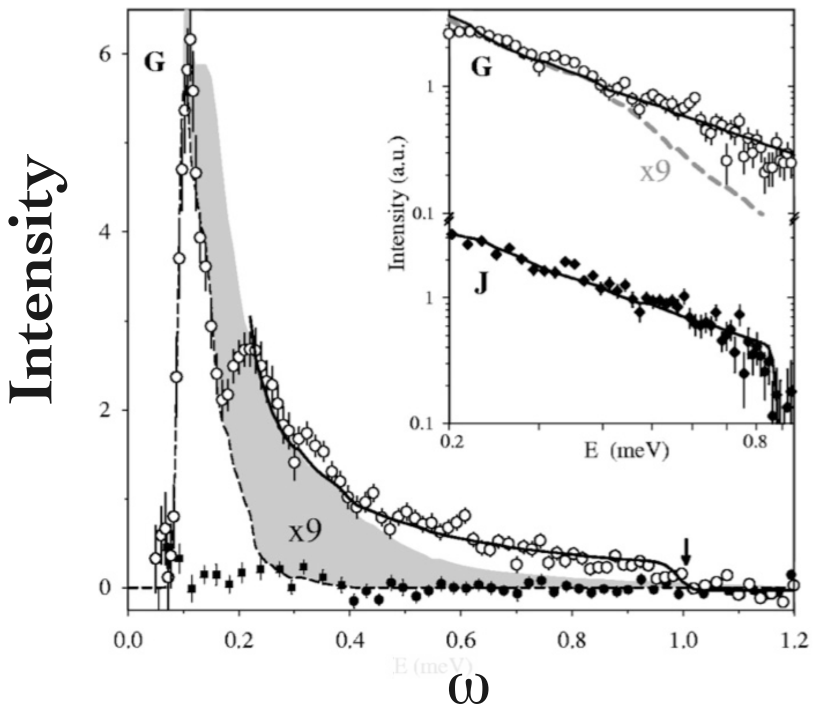

Dynamical structure factor $S(k, \omega)$ at $k_x=\pi$[1]

Spinon :

Power-law divergence with a large tail.

Magnon :

δ-functional peak with negligible tail.

[1] R.Coldea, *et al.*, Phys. Rev. B **68**, 134424 (2003).

Theoretical proposals for 2D spinons

- J.Alicea, O.I.Motrunich & M.P.Fisher: Phys. Rev. Lett. **95**, 247203 (2005).
- S.V.Isakov, T.Senthil & Y.B.Kim: Phys. Rev. B **72**, 174417 (2005).
- Y.Zhou & X.-G.Wen: cond-mat/0210662.
- F.Wang & A.Vishwanath: Phys. Rev. B **74**, 174423 (2006).
- C.-H.Chung, K.Voelker & Y. B. Kim: Phys. Rev. B **68**, 094412 (2003).

...

$$S(k,\omega) \propto \frac{1}{\left[\omega^2 - \omega_L(k_x)^2\right]^{1-\eta/2}},$$

$\eta=0.74\pm0.14$ (experimental fit)

2D Dispersion Relation in Cs_2CuCl_4

Dispersion relation in Cs_2CuCl_4

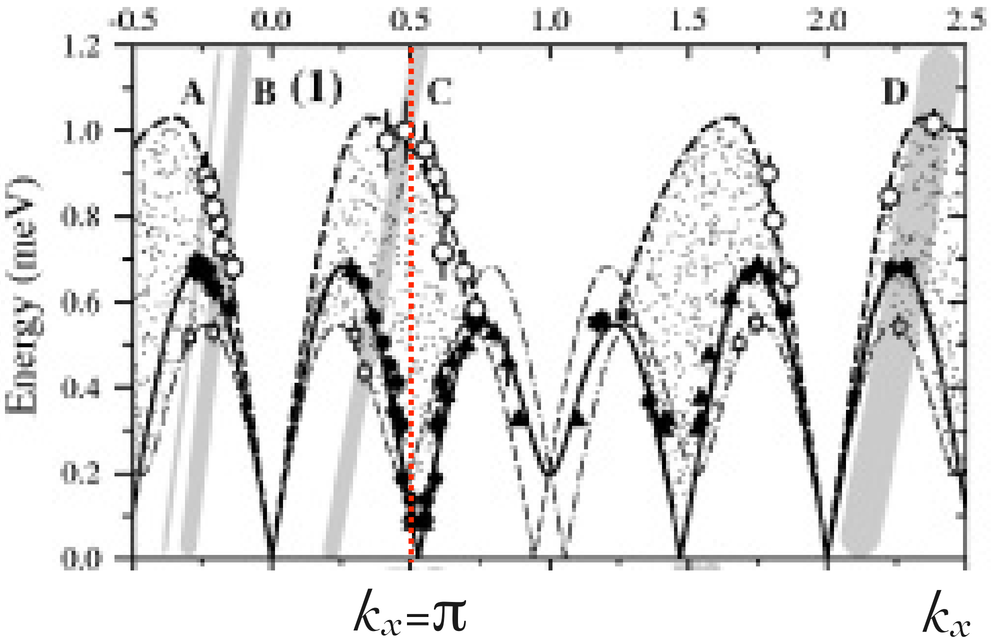

Asymmetry with respect to k_x=π
is due to interchain couplings.

[1] R.Coldea, *et al.*, Phys. Rev. B **68**, 134424 (2003).

Spin-wave theory

- M.Y.Veillette, A.J.A.James & F.H.L.Essler: Phys. Rev. B **72**, 134429 (2005).
- D.Dalidovich, R.Sknepnek, A.J.Berlinsky, J.Zhang & C.Kallin: Phys. Rev. B **73**, 184403 (2006).
- R.Coldea, D.A.Tennant & Z.Tylczynski: Phys. Rev. B **68**, 134424 (2003).

...

$$\omega_k = \sqrt{(J_k - J_Q)\left[(J_{k-Q} + J_{k+Q})/2 - J_Q\right]},$$

$$J_k = \tilde{J}\cos k'_x + 2\tilde{J}'\cos\frac{k'_x}{2}\cos\frac{k'_y}{2},$$

$\underline{\tilde{J} = 0.61(1)\text{meV}, \quad \tilde{J}' = 0.107(10)\text{meV}.}$

c.f. bare couplings

$\underline{J\text{=}0.374(5)\text{meV}, J'\text{=}0.128(5)\text{meV}.}$

Different Types of Line Shapes in Cs_2CuCl_4

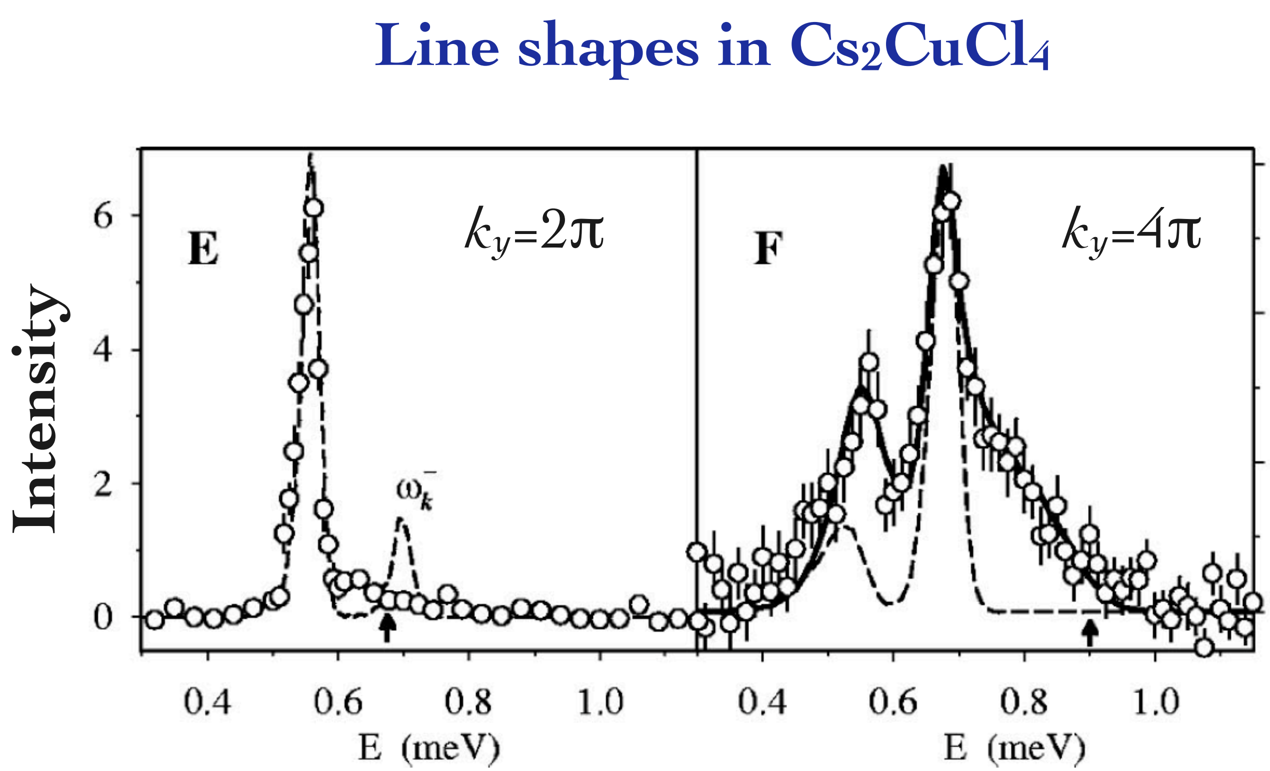

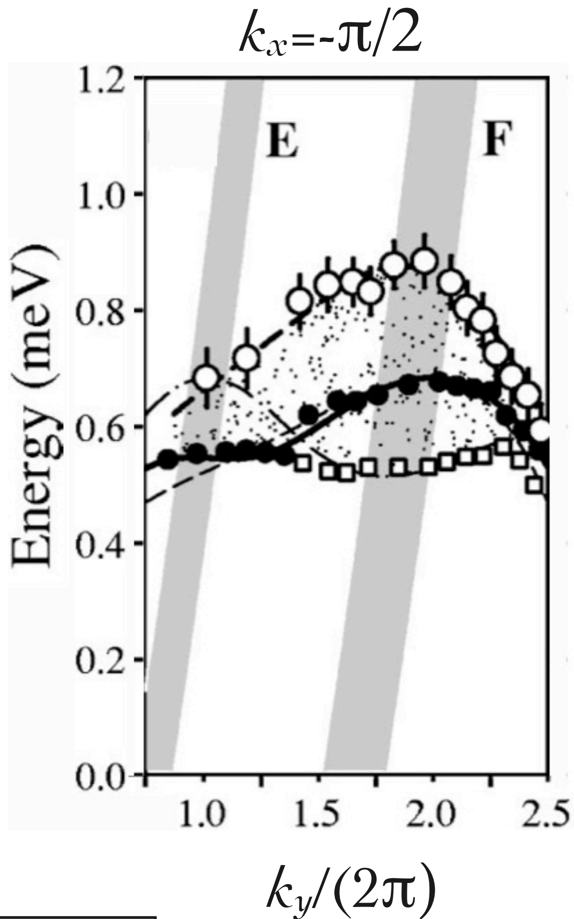

Depending on the momentum,
$S(\boldsymbol{k},\omega)$ can have a sharp peak or broad continuum.

R.Coldea, *et al*., Phys. Rev. B **68**, 134424 (2003).

Unusual Features in Cs_2CuCl_4

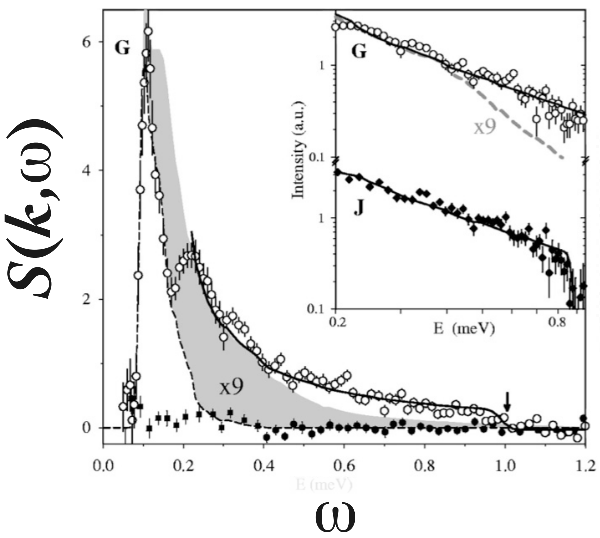

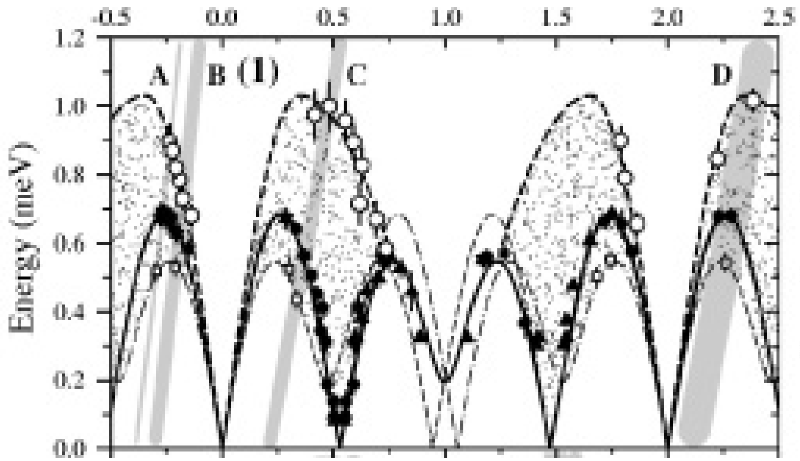

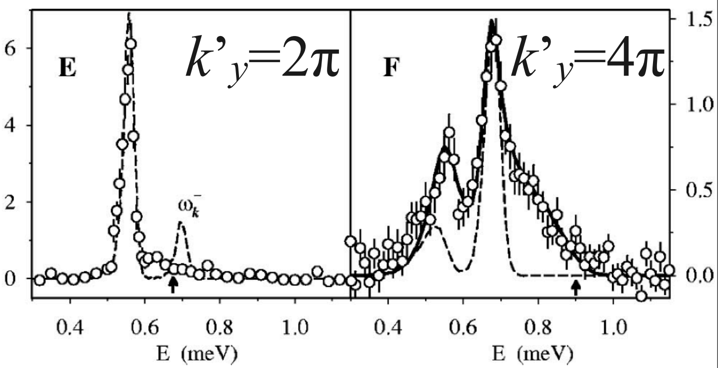

Large tail in $S(k,\omega)$
2D Spinon?

2D dispersion relation
Spin-wave theory?

Momentum dependence of line shape
???

R.Coldea, *et al*., Phys. Rev. B **68**, 134424 (2003).

Interpretation of experimental results is controversial.

Consistent explanation by a controlled approximation basically without fitting parameter

Model

Model

Spatially anisotropic ($J' < J$) spin-1/2 antiferromagnetic Heisenberg model ($J, J' > 0$).

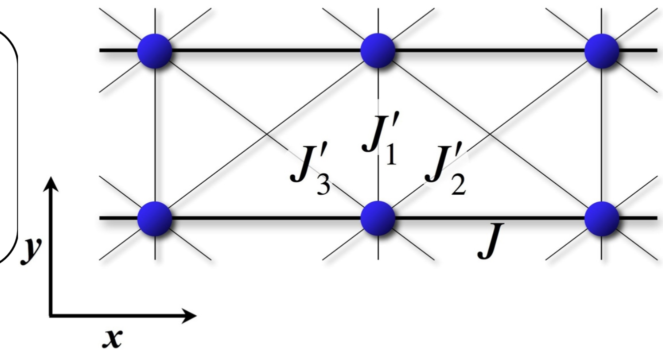

$$H = \sum_{x,y} \left(J\boldsymbol{S}_{x+1,y} + J'_1\boldsymbol{S}_{x,y+1} + J'_2\boldsymbol{S}_{x+1,y+1} + J'_3\boldsymbol{S}_{x-1,y+1} \right) \cdot \boldsymbol{S}_{x,y}.$$

[J : intra-chain coupling , J'_1, J'_2, J'_3 : inter-chain coupling]

Highly frustrated antiferromagets : $J'_1 = J'_2 + J'_3$.

Model

Model

Spatially anisotropic ($J' < J$) spin-1/2 antiferromagnetic Heisenberg model ($J, J' > 0$).

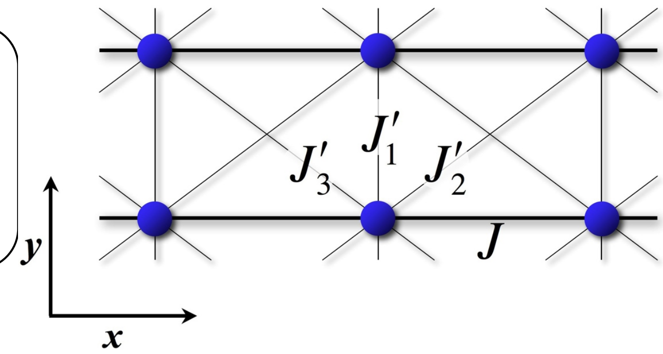

$$H = \sum_{x,y} \left(J\boldsymbol{S}_{x+1,y} + J'_1\boldsymbol{S}_{x,y+1} + J'_2\boldsymbol{S}_{x+1,y+1} + J'_3\boldsymbol{S}_{x-1,y+1} \right) \cdot \boldsymbol{S}_{x,y}.$$

[J : intra-chain coupling , J'_1, J'_2, J'_3 : inter-chain coupling]

Highly frustrated antiferromagets : $\boldsymbol{J'_1 = J'_2 + J'_3}$.

- Spatially anisotropic triangular lattice:

$J'_1 = J'_2$, $J'_3 = 0$

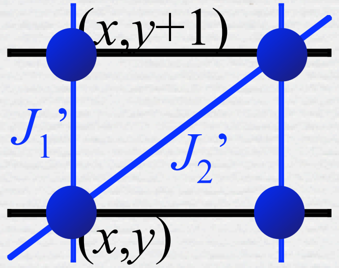

Model

Model

Spatially anisotropic ($J' < J$) spin-1/2 antiferromagnetic Heisenberg model ($J, J' > 0$).

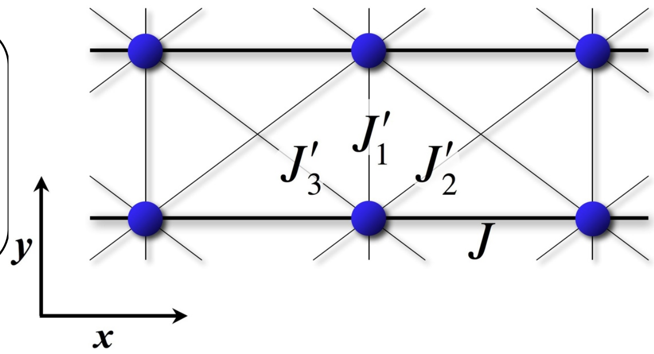

$$H = \sum_{x,y} \left(J\boldsymbol{S}_{x+1,y} + J'_1\boldsymbol{S}_{x,y+1} + J'_2\boldsymbol{S}_{x+1,y+1} + J'_3\boldsymbol{S}_{x-1,y+1} \right) \cdot \boldsymbol{S}_{x,y}.$$

[J : intra-chain coupling , J'_1, J'_2, J'_3 : inter-chain coupling]

Highly frustrated antiferromagets : $J'_1 = J'_2 + J'_3$.

- Spatially anisotropic triangular lattice:

$J'_1 = J'_2$, $J'_3 = 0$

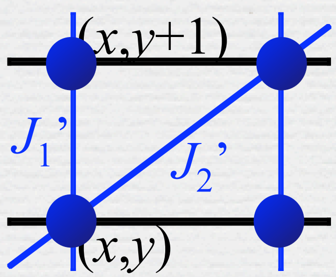

- Spatially anisotropic J_1-J_2 model:

$J'_2 = J'_3 = J'_1/2$: critical

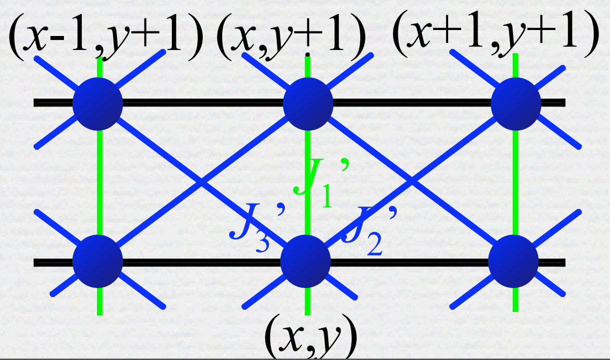

Decoupled Chain Limit ($J' \to 0$)

At $J'=0$, the system is decomposed into decoupled Heisenberg chains.

The S=1/2 Heisenberg chain is exactly solved by the Bethe ansatz.

$$\begin{cases} \text{Ground state : } S=0,\ E_0=J(-\ln 2+1/4)L \quad (L\text{:length}). \\ \text{Triplet states : 2-, 4-, ... spinon states} \end{cases}$$

Decoupled Chain Limit ($J' \to 0$)

At $J'=0$, the system is decomposed into decoupled Heisenberg chains.

The S=1/2 Heisenberg chain is exactly solved by the Bethe ansatz.

$$\begin{cases} \text{Ground state : } S=0,\ E_0=J(-\ln 2+1/4)L \quad (L\text{:length}). \\ \text{Triplet states : 2-, 4-, ... spinon states} \end{cases}$$

2-spinon states can be specified by 2 quasi-momenta (k_{x1}, k_{x2}).

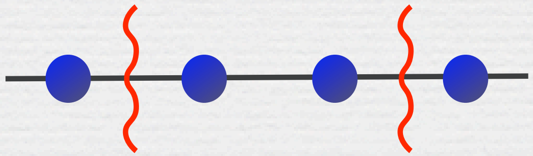

Alternatively, we can specify them by total momentum k_x and excitation energy ε_{kx}.

$$\begin{cases} k_x = k_{x1} + k_{x2} \\ \varepsilon_{kx} = \pi J \sin[k_x/2]\cos[(k_{x1}-k_{x2})/2] \end{cases}$$

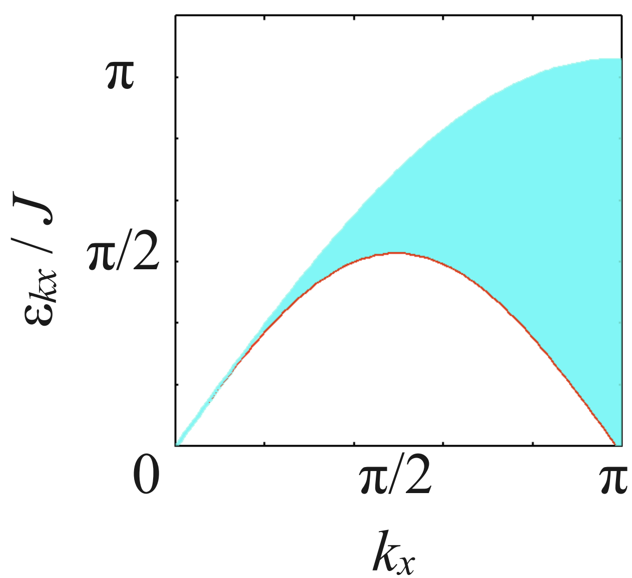

2-spinon spectrum of Heisenberg chain

Basis

At $J'=0$, exact ground state and triplet states are given as follows:

$$\left|\mathrm{G.S.}\right\rangle_0 = \bigotimes_y \left|0\right\rangle_y$$

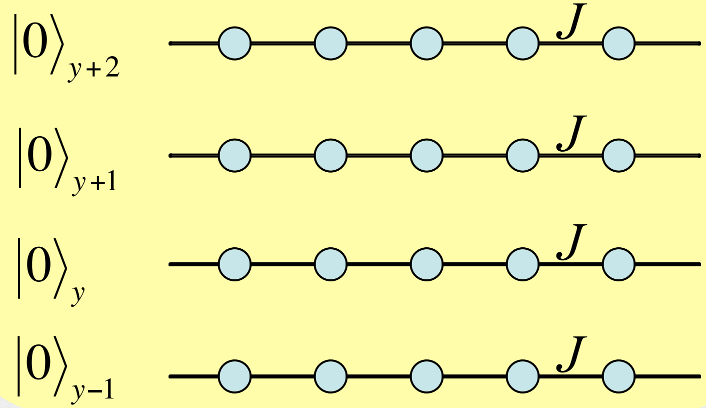

$$\left|k_x,\varepsilon_{k_x},y\right\rangle = \left|k_x,\varepsilon_{k_x}\right\rangle_y \bigotimes_{y'\neq y}\left|0\right\rangle_{y'}$$

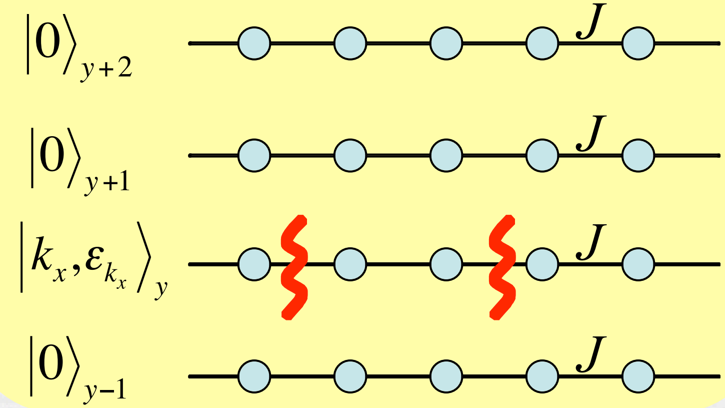

$\left|0\right\rangle_y$: Ground state of y-th chain.

$\left|k_x,\varepsilon_{k_x}\right\rangle_y$: 2-spinon state of y-th chain with $S=1$, momentum k_x and energy $\varepsilon_{kx}+E_0$.

Basis

At J'=0, exact ground state and triplet states are given as follows:

$$\left|\mathrm{G.S.}\right\rangle_0 = \bigotimes_y \left|0\right\rangle_y$$

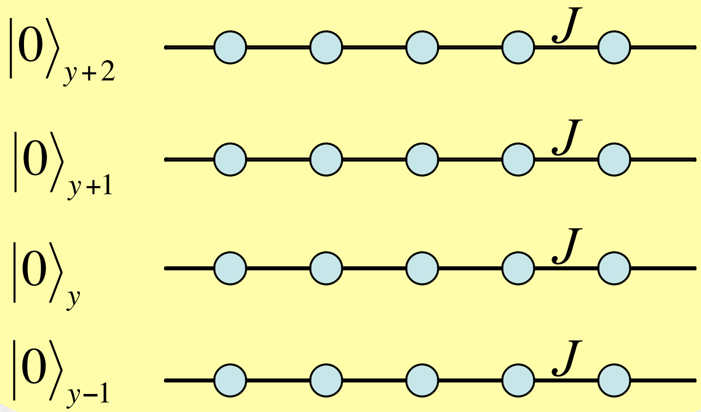

$|0\rangle_y$: Ground state of y-th chain.

$$\left|k_x,\varepsilon_{k_x},y\right\rangle = \left|k_x,\varepsilon_{k_x}\right\rangle_y \bigotimes_{y'\neq y} \left|0\right\rangle_{y'}$$

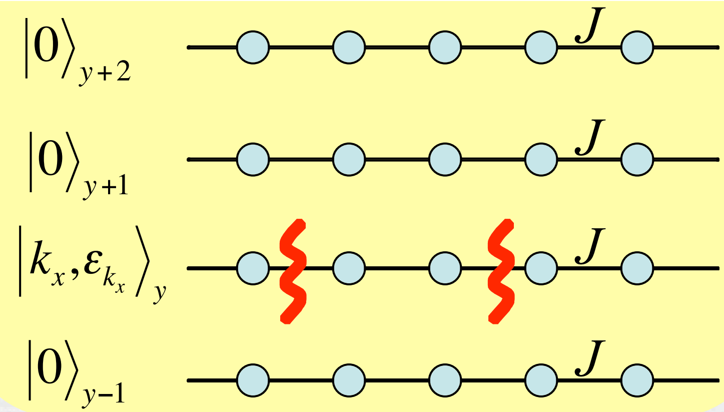

$\left|k_x,\varepsilon_{k_x}\right\rangle_y$: 2-spinon state of y-th chain

with S=1, momentum k_x and energy $\varepsilon_{kx}+E_0$.

In the small J' regime, restricting the Hilbert space to that spanned by this basis, states with momentum k_x and k_y are expressed as

$$\left|\psi\left(k_x,k_y\right)\right\rangle = \int d\varepsilon_{k_x} D_{k_x}\left(\varepsilon_{k_x}\right) c_{k_x,k_y}\left(\varepsilon_{k_x}\right) \left|k_x,\varepsilon_{k_x},k_y\right\rangle, \quad \left|k_x,\varepsilon_{k_x},k_y\right\rangle \equiv \frac{1}{\sqrt{L}}\sum_y \mathrm{e}^{\mathrm{i}k_y y}\left|k_x,\varepsilon_{k_x},y\right\rangle.$$

Interchain Interaction

Expressing spin operators in k-space, H_1 term is rewritten as follows:

$$H_1 = \sum_{k_x, y} J'(k_x) \boldsymbol{S}_{k_x, y} \cdot \boldsymbol{S}_{-k_x, y+1}, \quad J'(k_x) \equiv J'_1 + J'_2 \mathrm{e}^{\mathrm{i}k_x} + J'_3 \mathrm{e}^{-\mathrm{i}k_x}.$$

The expectation value of the interaction H_1 by $|\psi(k_x,k_y)>$ has terms like

y+2: $\quad {}_{y+2}\langle 0| \qquad |0\rangle_{y+2} \quad \rightarrow \quad 1$

y+1: $\quad {}_{y+1}\langle k_x, \varepsilon'_{k_x}| \ \boldsymbol{S}_{k_x, y+1} \ |0\rangle_{y+1} \quad \rightarrow \quad \langle k_x, \varepsilon'_{k_x} | \boldsymbol{S}_{k_x, y+1} | 0 \rangle = A^*(k_x, \varepsilon'_{k_x})$

y : $\quad {}_{y}\langle 0| \ \boldsymbol{S}_{-k_x, y} |k_x, \varepsilon_x\rangle_y \quad \rightarrow \quad \langle 0 | \boldsymbol{S}_{-k_x, y} | k_x, \varepsilon'_{k_x} \rangle = A(k_x, \varepsilon_{k_x})$

y-1 : $\quad {}_{y-1}\langle 0| \qquad |0\rangle_{y-1} \quad \rightarrow \quad 1$

$$A(k_x, \varepsilon_{k_x}) \equiv \langle 0 | S^{\alpha}_{-k_x, y} | k_x, \varepsilon_{k_x} \rangle_y$$

(α=x, y or z).

$$\langle \psi(k_x, k_y) | H_1 | \psi(k_x, k_y) \rangle$$

$$= J'(k_x, k_y) \int d\varepsilon_{k_x} \int d\varepsilon'_{k_x} D_{k_x}(\varepsilon_{k_x}) D_{k_x}(\varepsilon'_{k_x}) c^*_{k_x, k_y}(\varepsilon_{k_x}) c_{k_x, k_y}(\varepsilon'_{k_x}) A^*(k_x, \varepsilon_{k_x}) A(k_x, \varepsilon'_{k_x}),$$

where $\quad J'(k_x, k_y) \equiv 2\{J'_1 \cos k_y + J'_2 \cos(k_x + k_y) + J'_3 \cos(k_x - k_y)\}.$

Effective Hamiltonian for Small *J'*

$$\left\langle \psi(k_x,k_y) \middle| H \middle| \psi(k_x,k_y) \right\rangle = \sum_{i,j} \bar{c}^{*}_{k_x,k_y}\left(\varepsilon^i_{k_x}\right) H^{(k_x,k_y)}_{i,j} \bar{c}_{k_x,k_y}\left(\varepsilon^j_{k_x}\right), \quad \bar{c}_{k_x,k_y}\left(\varepsilon^j_{k_x}\right) \equiv \sqrt{\frac{k_x}{2M}} c_{k_x,k_y}\left(\varepsilon^j_{k_x}\right).$$

$$H^{(k_x,k_y)}_{i,j} = \left(\varepsilon^i_{k_x} + E_0 L\right)\delta_{i,j} + \frac{k_x}{2M} J'(k_x,k_y) A^*\left(k_x,\varepsilon^i_{k_x}\right) A\left(k_x,\varepsilon^j_{k_x}\right),$$

where

$$\begin{cases} J'(k_x,k_y) \equiv 2\left\{J'_1 \cos k_y + J'_2 \cos(k_x + k_y) + J'_3 \cos(k_x - k_y)\right\} \\ A\left(k_x,\varepsilon_{k_x}\right) \equiv \left\langle 0 \middle| S^{\alpha}_{-k_x,y} \middle| k_x,\varepsilon_{k_x} \right\rangle_y \end{cases}$$

($\alpha = x, y$ or z)

(M is the number of points in the ω space.)

Effective Hamiltonian for Small J'

$$\left\langle \psi(k_x,k_y) \middle| H \middle| \psi(k_x,k_y) \right\rangle = \sum_{i,j} \bar{c}^{*}_{k_x,k_y}\left(\varepsilon^{i}_{k_x}\right) H^{(k_x,k_y)}_{i,j} \bar{c}_{k_x,k_y}\left(\varepsilon^{j}_{k_x}\right), \quad \bar{c}_{k_x,k_y}\left(\varepsilon^{j}_{k_x}\right) \equiv \sqrt{\frac{k_x}{2M}} c_{k_x,k_y}\left(\varepsilon^{j}_{k_x}\right).$$

$$H^{(k_x,k_y)}_{i,j} = \left(\varepsilon^{i}_{k_x} + E_0 L\right)\delta_{i,j} + \frac{k_x}{2M} J'(k_x,k_y) A^{*}\left(k_x,\varepsilon^{i}_{k_x}\right) A\left(k_x,\varepsilon^{j}_{k_x}\right),$$

where
$$\begin{cases} J'(k_x,k_y) \equiv 2\left\{ J'_1 \cos k_y + J'_2 \cos(k_x + k_y) + J'_3 \cos(k_x - k_y) \right\} \\ A\left(k_x,\varepsilon_{k_x}\right) \equiv \left\langle 0 \middle| S^{\alpha}_{-k_x,y} \middle| k_x,\varepsilon_{k_x} \right\rangle_y \end{cases}$$

(α=x,y or z)

(M is the number of points in the ω space.)

Dynamical structure factor $S(k,\omega)$ is obtained as

$$S(k,\omega) \cong \sum_i \left| \left\langle \mathrm{G.S.} \middle| S^{\alpha}_{-k} \middle| i(k) \right\rangle \right|^2 \delta\left(\omega - e_i(k)\right),$$

where
$$\left| \left\langle k_x, e^{i}_{k_x,k_y}, k_y \middle| S^{\alpha}_{k_x,k_y} \middle| \mathrm{G.S.} \right\rangle \right|^2 \cong \left| \sum_j \bar{c}^{i*}_{k_x,k_y}\left(\varepsilon^{j}_{k_x}\right) A^{*}\left(k_x,\varepsilon^{j}_{k_x}\right) \left\{ 1 - J'(k_x,k_y) \sum_l \frac{k_x}{2M} \frac{\left| A\left(-k_x,\varepsilon^{l}_{-k_x}\right) \right|^2}{\varepsilon^{j}_{k_x} + \varepsilon^{l}_{-k_x}} \right\} \right|^2 .$$

Transition Rate in the Heisenberg Chain

The transition rate $M(k,\omega)$ between the ground state and 2-spinon states is exactly obtained for the Heisenberg chain by an algebraic analysis based on the (infinite-dimensional symmetry) quantum group[2]:

$$A\left(k_x,\varepsilon_{k_x}\right) = \sqrt{M\left(k_x,\varepsilon_{k_x}\right)},$$

$$M\left(k_x,\varepsilon_{k_x}\right) \equiv \left|\left\langle 0\left|S^{\alpha}_{-k_x}\right|k_x,\varepsilon_{k_x}\right\rangle\right|^2 = \frac{1}{4\pi}\exp\left(-\int_0^\infty dx\,\frac{\cosh(2x)\cos(xt)-1}{x\sinh(2x)\cosh(x)}\mathrm{e}^{x}\right),$$

where $$t = \frac{4}{\pi}\ln\left(\frac{\sqrt{{\omega_U^{k_x}}^2-{\omega_L^{k_x}}^2}+\sqrt{{\omega_U^{k_x}}^2-{\varepsilon_{k_x}}^2}}{\sqrt{{\varepsilon_{k_x}}^2-{\omega_L^{k_x}}^2}}\right),$$

$$\omega_U^{k_x} = \pi J\sin\frac{k_x}{2},\quad \omega_L^{k_x} = \frac{\pi J}{2}\sin k_x.$$

[2] A.H. Bougourzi, M. Couture and M. Kacir, PRB **54**, R12669 (1996).

Effective Schrödinger Equation for Small J'

Alternatively,

$$\varepsilon_{k_x}\psi_{k_x}\left(\varepsilon_{k_x}\right)+J'(k)\int d\varepsilon'_{k_x}D\left(\varepsilon_{k_x}\right)A^{*}_{k_x}\left(\varepsilon_{k_x}\right)A_{k_x}\left(\varepsilon'_{k_x}\right)\psi_{k_x}\left(\varepsilon'_{k_x}\right)=e_k\psi_{k_x}\left(\varepsilon_{k_x}\right).$$

Effective Schrödinger Equation for Small J'

Alternatively,

$$\varepsilon_{k_x}\psi_{k_x}\left(\varepsilon_{k_x}\right)+J'(k)\int d\varepsilon'_{k_x}D\left(\varepsilon_{k_x}\right)A^*_{k_x}\left(\varepsilon_{k_x}\right)A_{k_x}\left(\varepsilon'_{k_x}\right)\psi_{k_x}\left(\varepsilon'_{k_x}\right)=e_k\psi_{k_x}\left(\varepsilon_{k_x}\right).$$

This equation can be solved analytically, and $S(k,\omega)$ is obtained as

$$S(k,\omega)=\frac{S_{1D}\left(k_x,\omega\right)}{\left[1+J'(k)\chi'_{1D}\left(k_x,\omega\right)\right]^2+\left[\pi J'(k)S_{1D}\left(k_x,\omega\right)\right]^2},$$

where $\chi'_{1D}\left(k_x,\omega\right)=\int_0^\infty d\omega'\frac{S_{1D}\left(k_x,\omega'\right)}{\omega'-\omega},\quad S_{1D}\left(k_x,\omega\right)=D_{k_x}(\omega)\left|A_{k_x}(\omega)\right|^2.$

This result is similar to RPA: $\operatorname{Re}\chi_{1D}\left(k_x,\omega\right)=\int_{-\infty}^\infty d\omega'\frac{S_{1D}\left(k_x,\left|\omega'\right|\right)}{\omega'-\omega}.$

Features of $S(\boldsymbol{k},\omega)$

$J'(k_x,k_y) = 0$

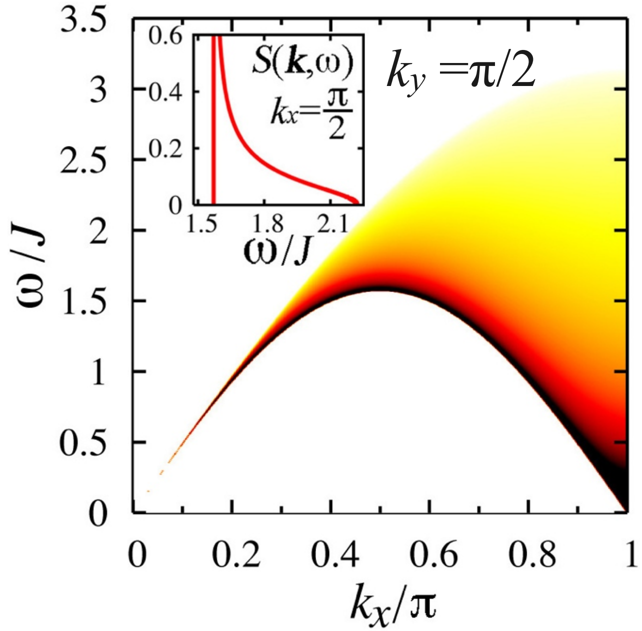

Interchain interactions effectively vanish. 1D spinons persist:

$$S(k,\omega) \propto \sqrt{\frac{-\ln\left(\omega-\omega_L\left(k_x\right)\right)}{\omega^2-\omega_L\left(k_x\right)^2}}$$

near $\omega \simeq \omega_L(k_x)$.

Spatially anisotropic J_1-J_2 model with $J'_2=J'_3=J'_1/2=0.24J$

Features of $S(\boldsymbol{k},\omega)$

$J'(k_x,k_y) < 0$

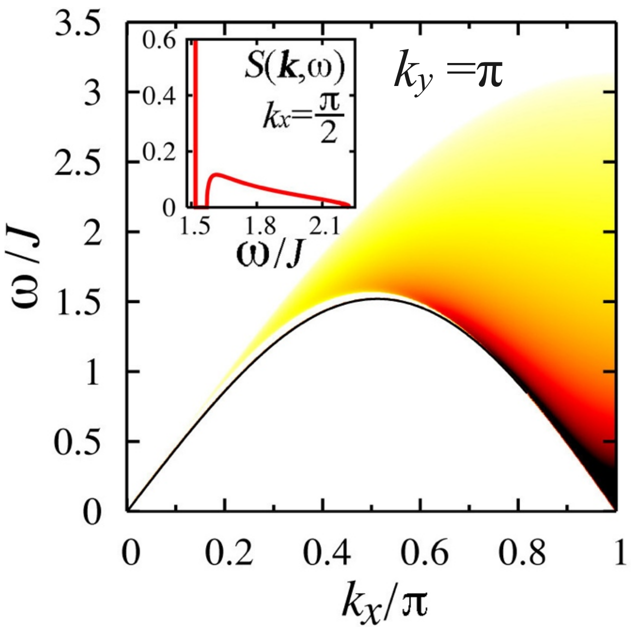

$J'(k_x,k_y) = 0$

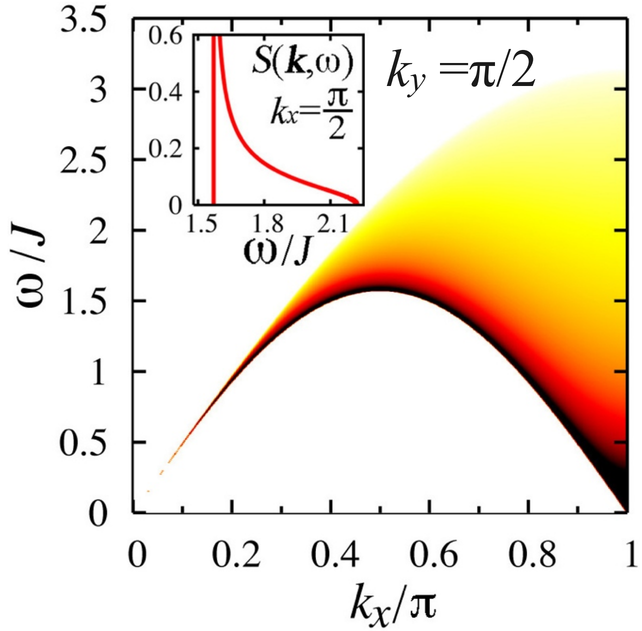

Bound state of spinons appear below continuum. It is similar to magnon, but does not require ordered ground states. It will be continuously connected to magnon.

Interchain interactions effectively vanish. 1D spinons persist:

$$S(k,\omega) \propto \sqrt{\frac{-\ln\left(\omega - \omega_L(k_x)\right)}{\omega^2 - \omega_L(k_x)^2}}$$

near $\omega \simeq \omega_L(k_x)$.

Spatially anisotropic J_1-J_2 model with $J'_2 = J'_3 = J'_1/2 = 0.24J$

Features of $S(\boldsymbol{k},\omega)$

$J'(k_x,k_y) < 0$ | $J'(k_x,k_y) = 0$ | $J'(k_x,k_y) > 0$

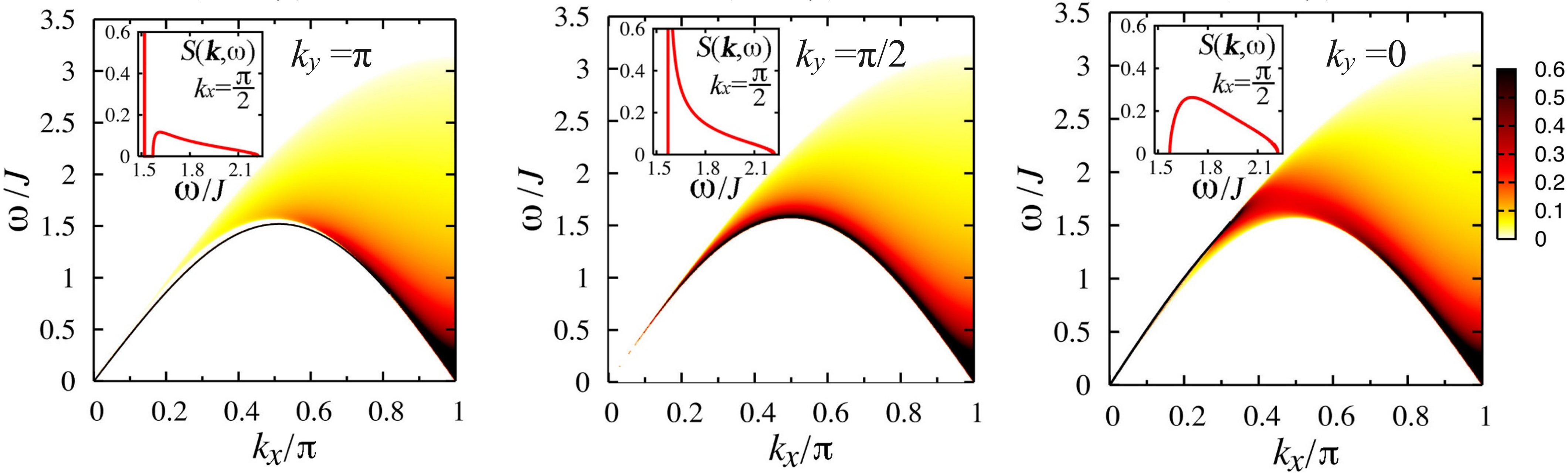

Bound state of spinons appear below continuum. It is similar to magnon, but does not require ordered ground states. It will be continuously connected to magnon.

Interchain interactions effectively vanish. 1D spinons persist:

$$S(k,\omega) \propto \sqrt{\frac{-\ln\left(\omega-\omega_L(k_x)\right)}{\omega^2-\omega_L(k_x)^2}}$$

near $\omega \simeq \omega_L(k_x)$.

Spectral weight shifts upwards. The peak is broadened in continuum. Anti-bound state appears above the 2-spinon continuum for small k_x.

Spatially anisotropic J_1-J_2 model with $J'_2=J'_3=J'_1/2=0.24J$

Bound State in RPA

The bound state is also obtained by RPA as a pole of dynamical susceptibility:

$$\mathrm{Re}\left[\chi_{2d}{}^{-1}(k,\omega)\right] = \mathrm{Re}\left[\chi_{1d}{}^{-1}(k,\omega)\right] + J'(k) = 0.$$

From this relation, the energy gap opens as $\Delta E \propto J'^2$ with logarithmic

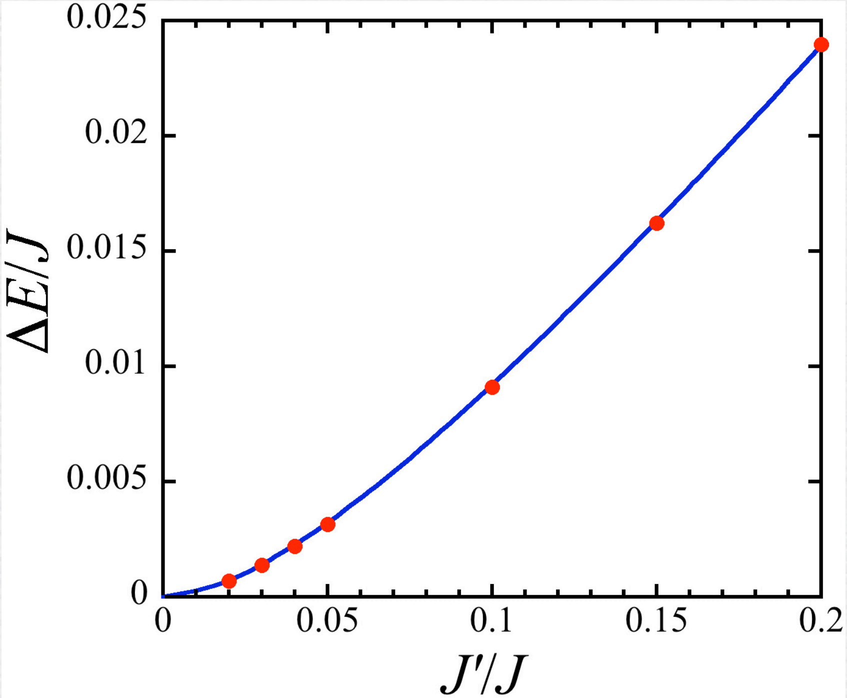

Energy gap ΔE between bound state and lower edge of continuum on a spatially anisotropic triangular lattice at k=(π/4,π).

● : present approach

—: RPA

Bound State in the Ising Limit

In the continuum, spinons are dispersed: $|\uparrow\downarrow\cdots\uparrow\downarrow\uparrow\wr\uparrow\downarrow\cdots\uparrow\downarrow\uparrow\wr\uparrow\downarrow\cdots\uparrow\downarrow\rangle.$

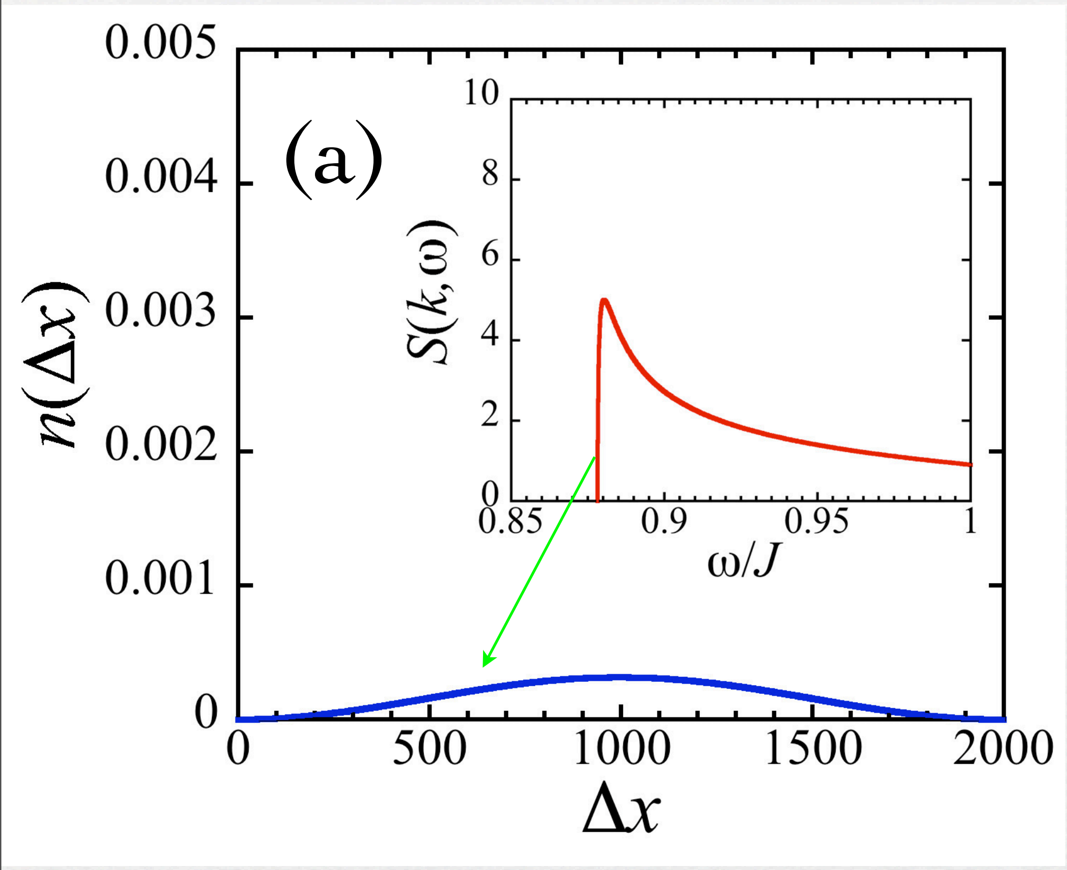

Density-density correlation function $n(\Delta x)$ in the lowest-energy state of the XXZ model in the Ising limit on a spatially anisotropic triangular lattice. (a) Incoherent state at k_x=0.708π and (b) bound state at k_x=0.667π.

Bound State in the Ising Limit

In the continuum, spinons are dispersed: $|\uparrow\downarrow\cdots\uparrow\downarrow\uparrow\;\uparrow\downarrow\cdots\uparrow\downarrow\uparrow\;\uparrow\downarrow\cdots\uparrow\downarrow\rangle.$

In the bound state, spinons are close to each other (Δx~0): $|\uparrow\downarrow\cdots\downarrow\uparrow\;\uparrow\;\uparrow\downarrow\cdots\uparrow\downarrow\rangle.$

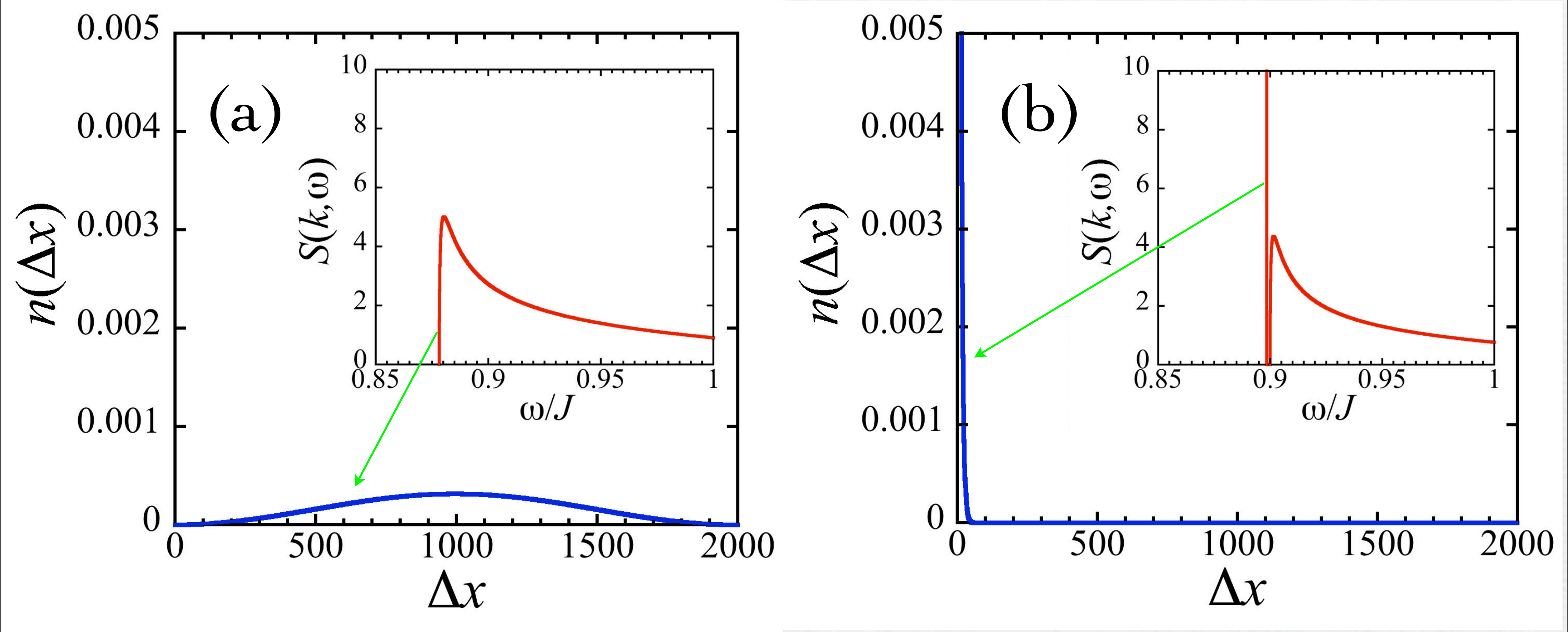

Density-density correlation function $n(\Delta x)$ in the lowest-energy state of the XXZ model in the Ising limit on a spatially anisotropic triangular lattice. (a) Incoherent state at k_x=0.708π and (b) bound state at k_x=0.667π.

Cs_2CuCl_4

Spatially anisotropic triangular lattice

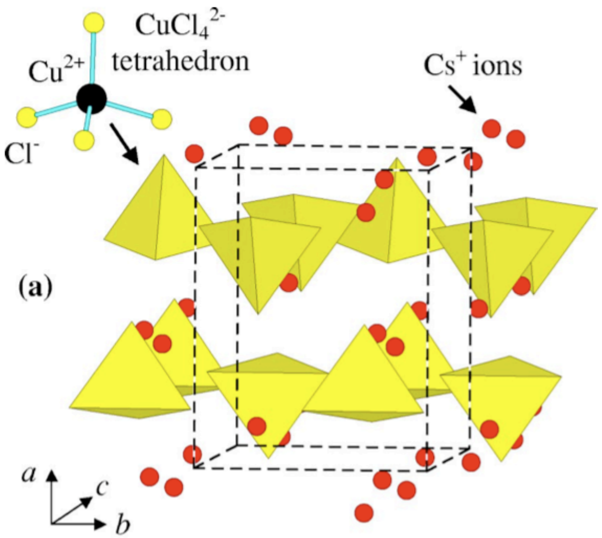

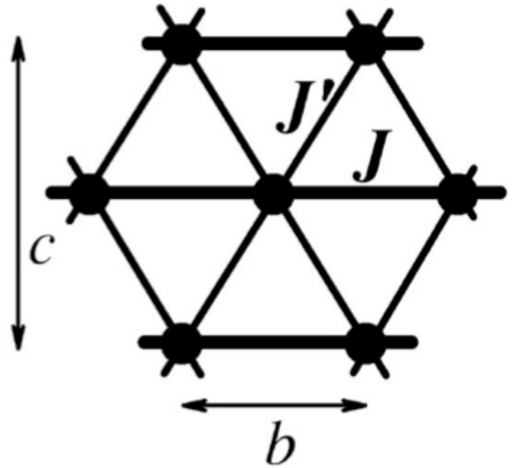

J=0.374(5)meV, J'=0.128(5)meV

J'/J=0.34(3)

(Interlayer J'' and DM ~ 0.05J)

R.Coldea, *et al*., PRL **86** 1335 (2001); PRB **68**, 134424 (2003).

Cs_2CuCl_4

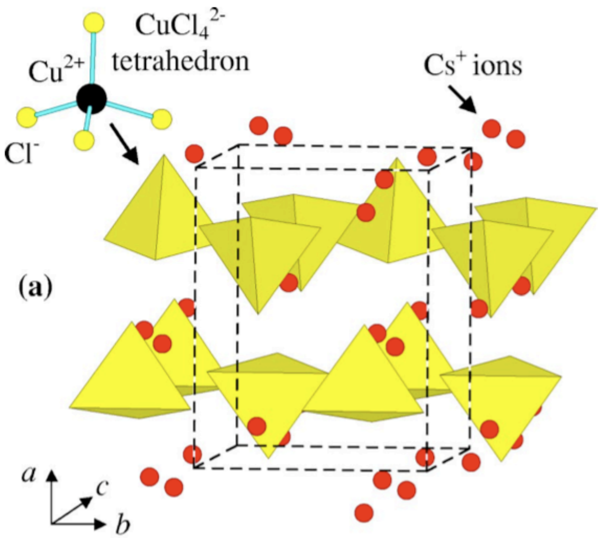

Spatially anisotropic triangular lattice

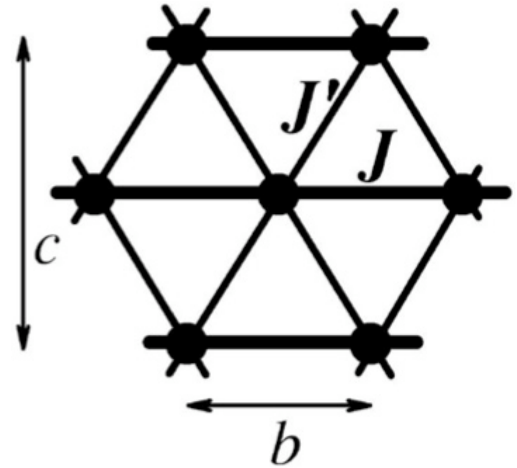

J=0.374(5)meV, J'=0.128(5)meV

J'/J=0.34(3)

(Interlayer J'' and DM ~ 0.05J)

$$\begin{cases} k'_x = k_x \\ k'_y = k_x + 2k_y \end{cases}$$

$$J'(k_x, k_y) = 4J'\cos\left(\frac{k'_x}{2}\right)\cos\left(\frac{k'_y}{2}\right).$$

Sign of $J'(\boldsymbol{k})$

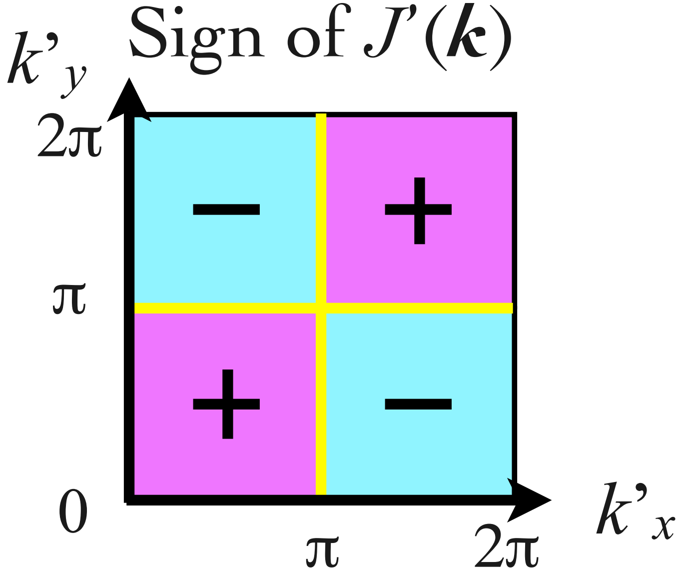

R.Coldea, *et al.*, PRL **86** 1335 (2001); PRB **68**, 134424 (2003).

Unusual Features Observed in Cs_2CuCl_4 by Coldea, *et al.*

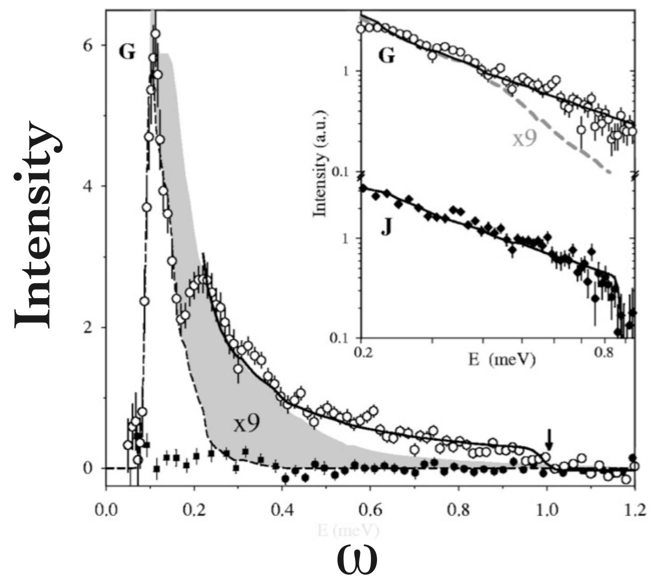

Large tail in $S(k,\omega)$ at $k'_x=\pi$
Similar to 1D spinons

R.Coldea, *et al.*, PRL **86** 1335 (2001); PRB **68**, 134424 (2003).

Unusual Features Observed in Cs_2CuCl_4 by Coldea, *et al.*

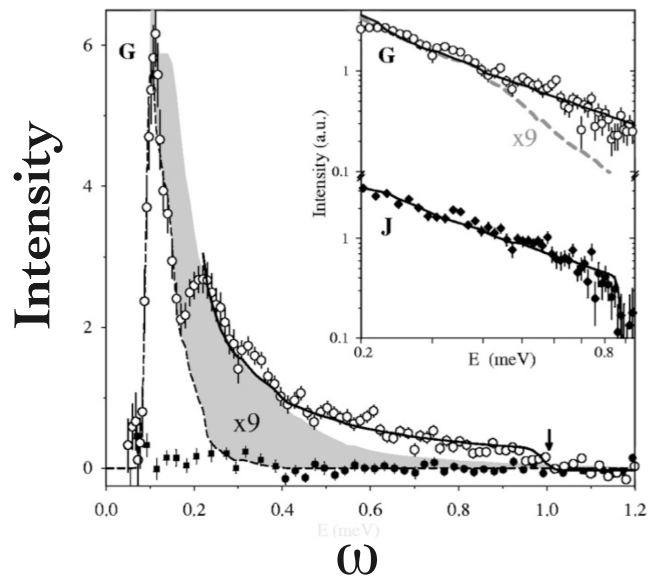

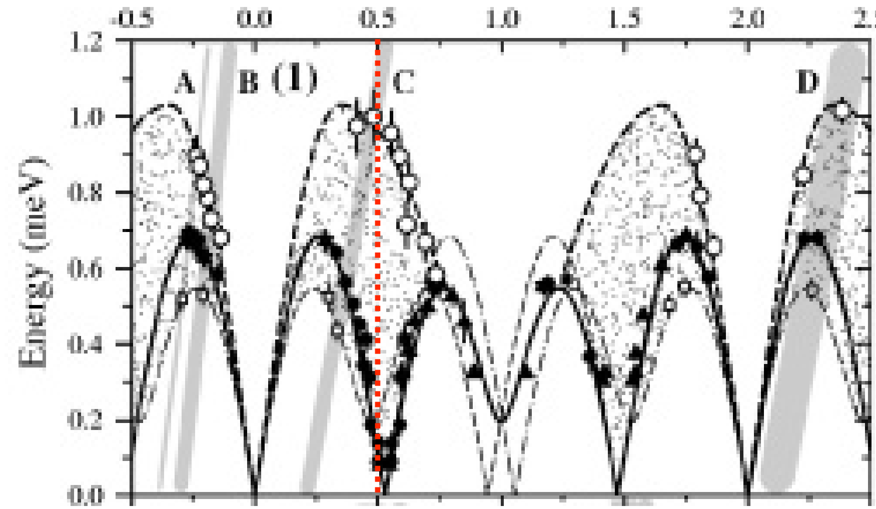

Large tail in $S(k,\omega)$ at $k'_x=\pi$
Similar to 1D spinons

2D dispersion relation
Asymmetry with respect to $k'_x=\pi$

R.Coldea, *et al.*, PRL **86** 1335 (2001); PRB **68**, 134424 (2003).

Unusual Features Observed in Cs_2CuCl_4 by Coldea, *et al.*

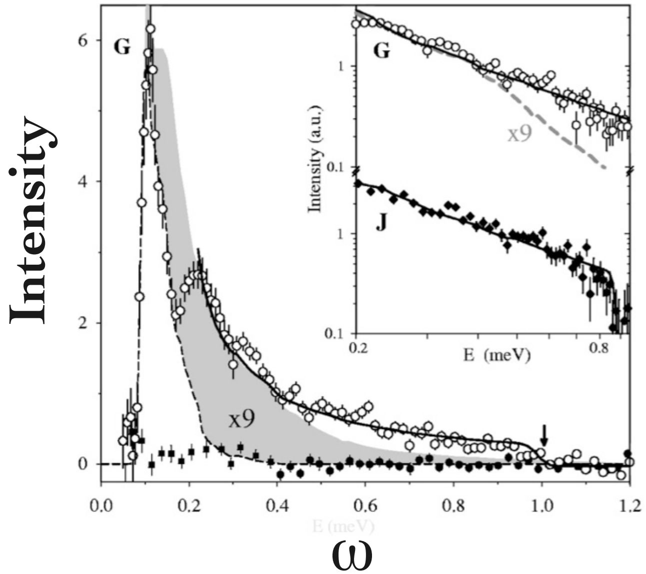

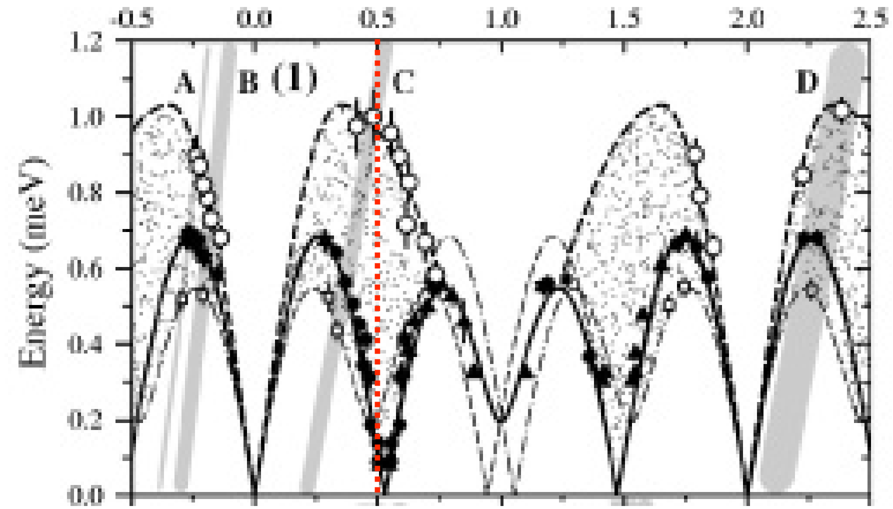

Large tail in $S(k,\omega)$ at $k'_x=\pi$
Similar to 1D spinons

2D dispersion relation
Asymmetry with respect to $k'_x=\pi$

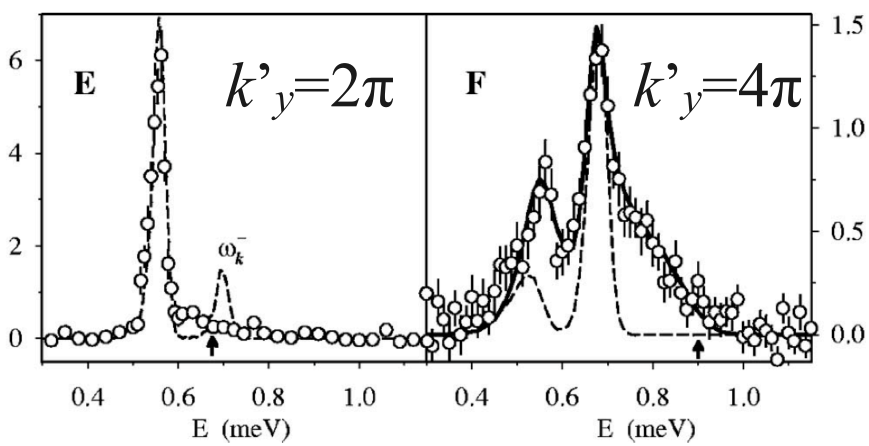

Strong momentum dependence of line shape

R.Coldea, *et al.*, PRL **86** 1335 (2001); PRB **68**, 134424 (2003).

Large Tail at $k'_x = \pi$

At $k'_x=\pi$, $S(\boldsymbol{k},\omega)$ reduces to that of the Heisenberg chain in the present approach,

because $J'(\boldsymbol{k})=0$. $$J'(k_x,k_y) = 4J'\cos\left(\frac{k'_x}{2}\right)\cos\left(\frac{k'_y}{2}\right).$$

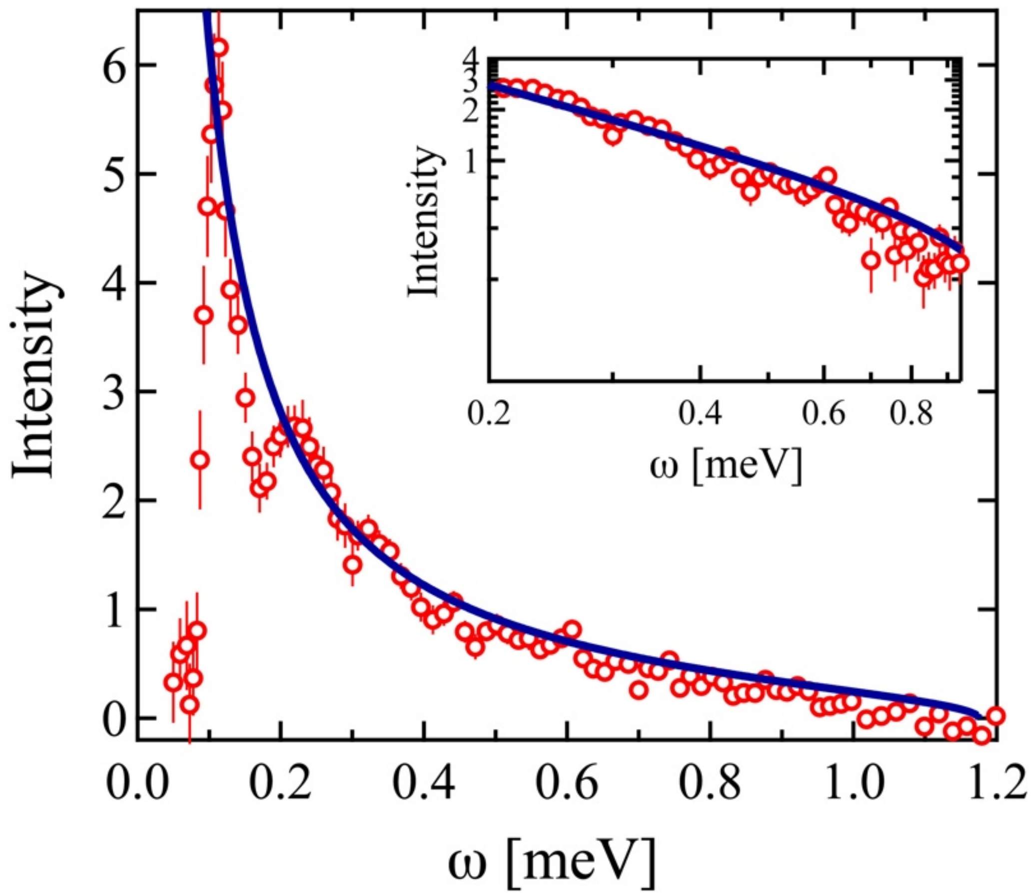

— : Present result

o : Experimental result of Cs_2CuCl_4 by Coldea, *et al*.[1]

Inset: log-log plot.

There is only one fitting parameter for the overall scale of intensity.
[This parameter is inevitable.]

$$S(k,\omega) \propto \sqrt{\frac{-\ln(\omega-\omega_L(k_x))}{\omega^2-\omega_L(k_x)^2}}$$ near $\omega \simeq \omega_L(k_x)$.

Comparison with Power-Law Fit

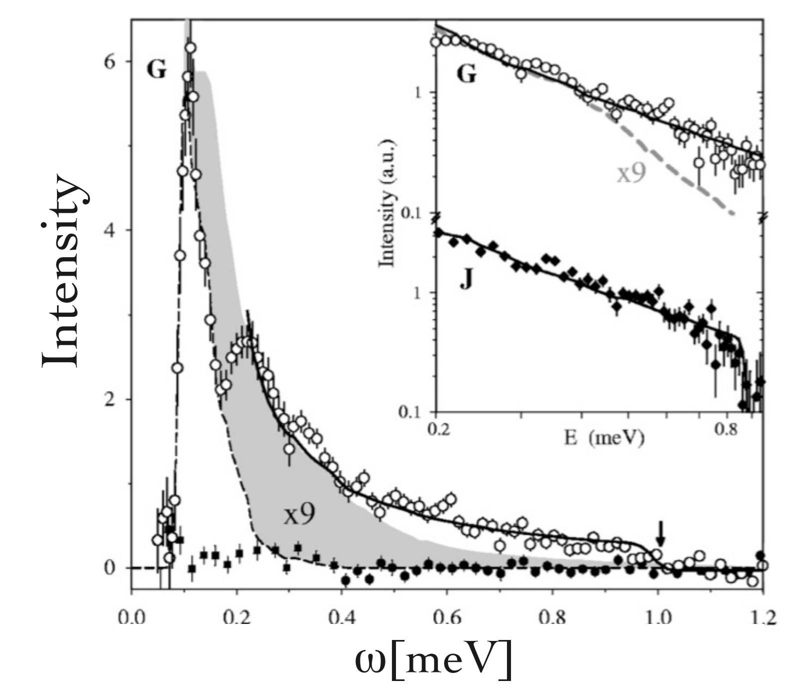

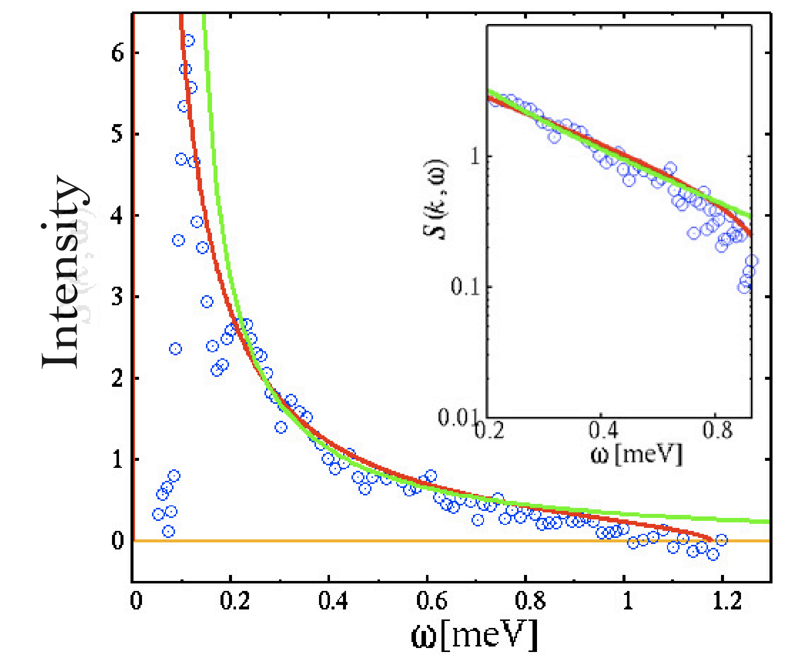

The experimental data at k_x=π have been fitted in a power-law form as

$$S(k,\omega) \propto \frac{1}{\left[\omega^2 - \omega_L(k_x)^2\right]^{1-\eta/2}},$$

where $\omega_L(k_x)$: lower edge of continuum.

$\eta = 0.74 \pm 0.14$

: Heisenberg chain (2-spinon)
: power-law fit with η=0.74
: experimental data[1]

Dispersion Relation along k'_x

At $k'_y=0$ and $k'_y=2\pi$, dispersion relation is asymmetric with respect to $k'_x=\pi$.

At $k'_y=3\pi$, dispersion relation is symmetric, because $J'(k'_x,k'_y=3\pi)=0$.

No fitting parameter

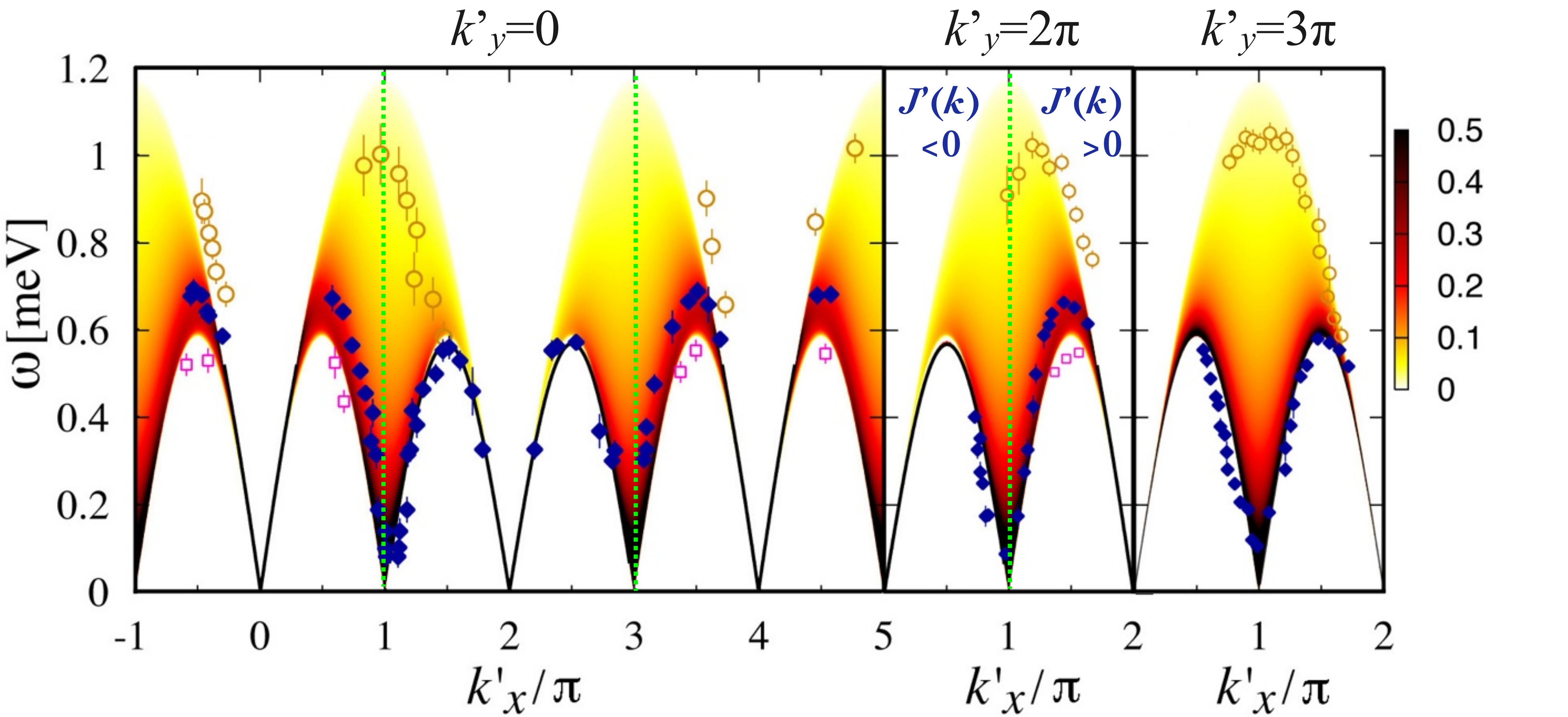

$$J'\left(k_x,k_y\right)=4J'\cos\left(\frac{k'_x}{2}\right)\cos\left(\frac{k'_y}{2}\right).$$

Main peak(♦), upper edge(○) and lower edge(□) estimated experimentally by Coldea, *et al.*[1].

Dispersion Relation along k'_x

At $k'_y=0$ and $k'_y=2\pi$, dispersion relation is asymmetric with respect to $k'_x=\pi$.

At $k'_y=3\pi$, dispersion relation is symmetric, because $J'(k'_x,k'_y=3\pi)=0$.

No fitting parameter

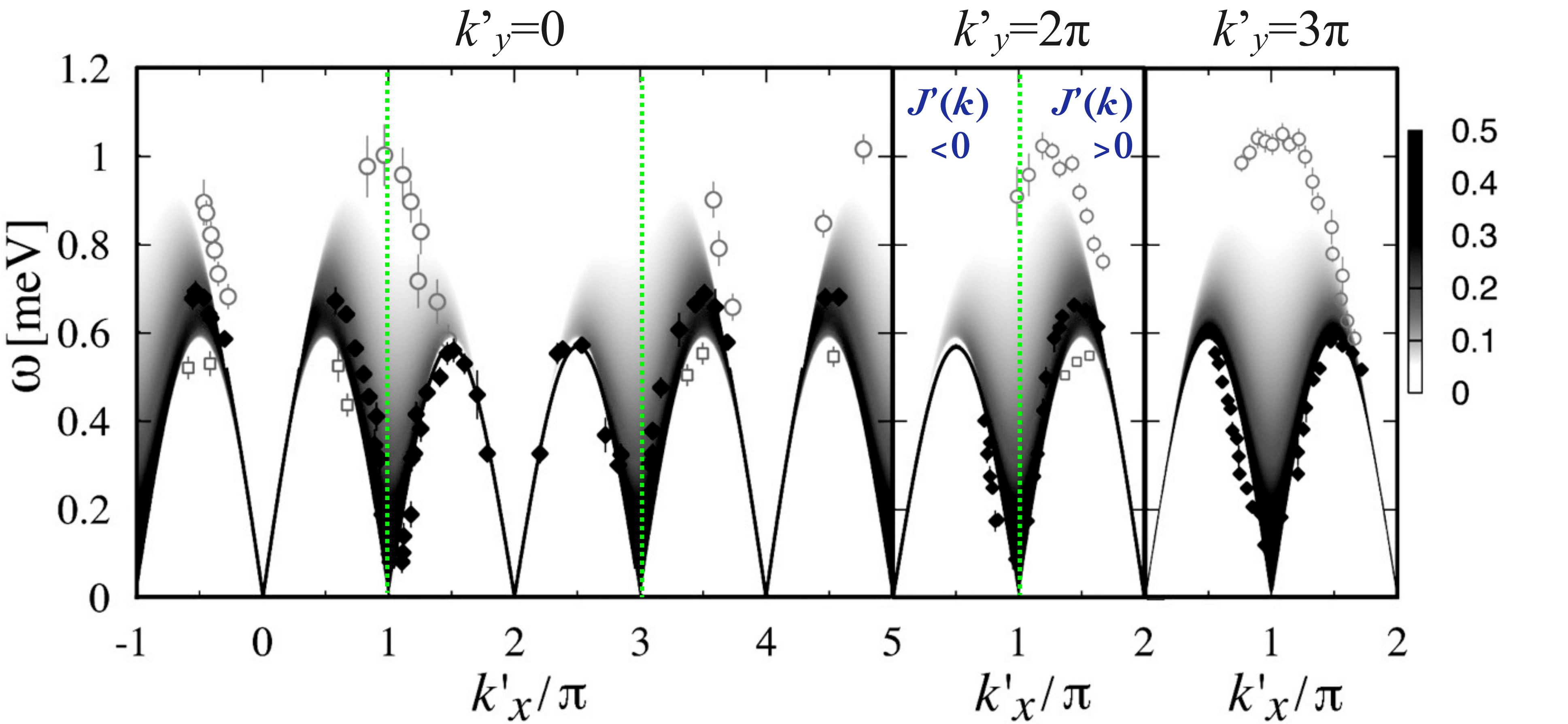

$$J'\left(k_x,k_y\right)=4J'\cos\left(\frac{k'_x}{2}\right)\cos\left(\frac{k'_y}{2}\right).$$

Main peak(◆), upper edge(○) and lower edge(□) estimated experimentally by Coldea, *et al.*[1].

Dispersion Relation along k'_y

At $k'_x=-\pi/2$, the sign of $J'(\boldsymbol{k})$ changes at $k'_y=3\pi$. No fitting parameter

For $k'_y<3\pi$ [$J'(\boldsymbol{k})<0$], a bound state is formed below the continuum.

For $k'_y>3\pi$ [$J'(\boldsymbol{k})>0$], the peak is broadened in the continuum.

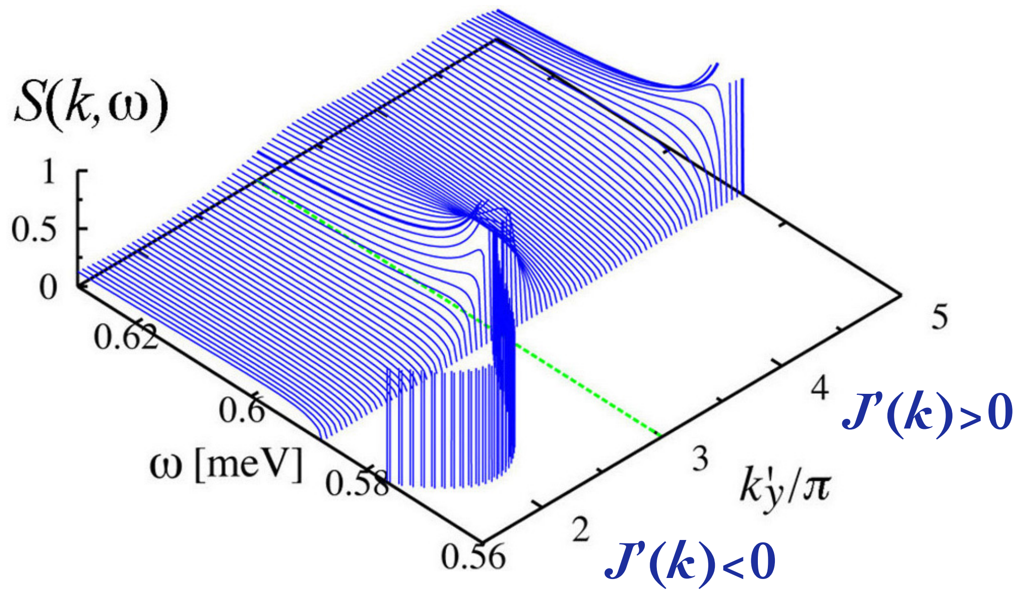

$S(k,\omega)$ at $k'_x=-\pi/2$ near the lower edge of the continuum by the present method.

$$J'(k_x,k_y)=4J'\cos\left(\frac{k'_x}{2}\right)\cos\left(\frac{k'_y}{2}\right).$$

Dispersion Relation along k'_y

At $k'_x = -\pi/2$, the sign of $J'(\boldsymbol{k})$ changes at $k'_y = 3\pi$. No fitting parameter

For $k'_y < 3\pi$ [$J'(\boldsymbol{k}) < 0$], a bound state is formed below the continuum.

For $k'_y > 3\pi$ [$J'(\boldsymbol{k}) > 0$], the peak is broadened in the continuum.

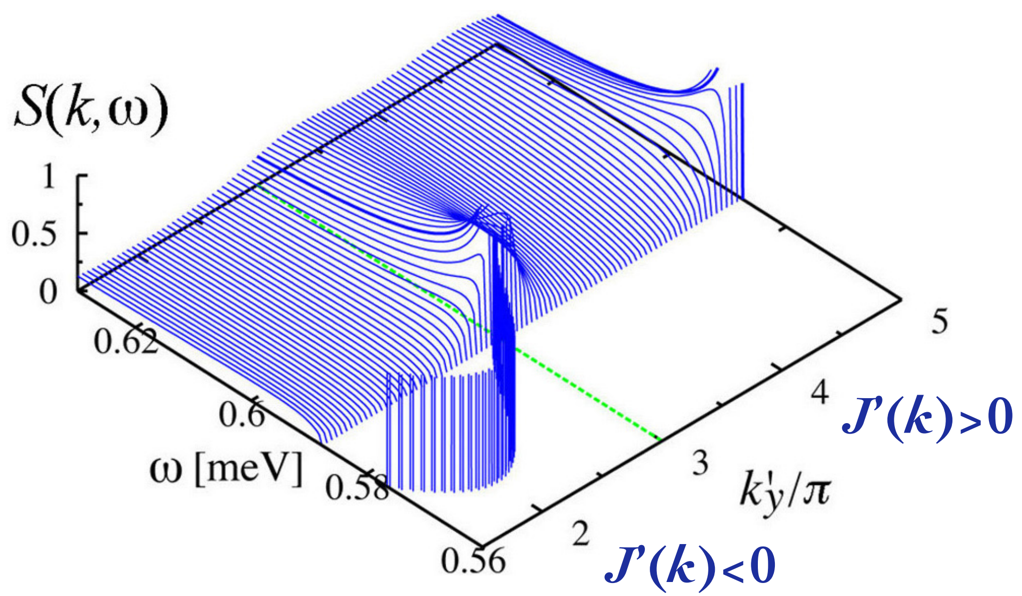

$S(k,\omega)$ at $k'_x = -\pi/2$ near the lower edge of the continuum by the present method.

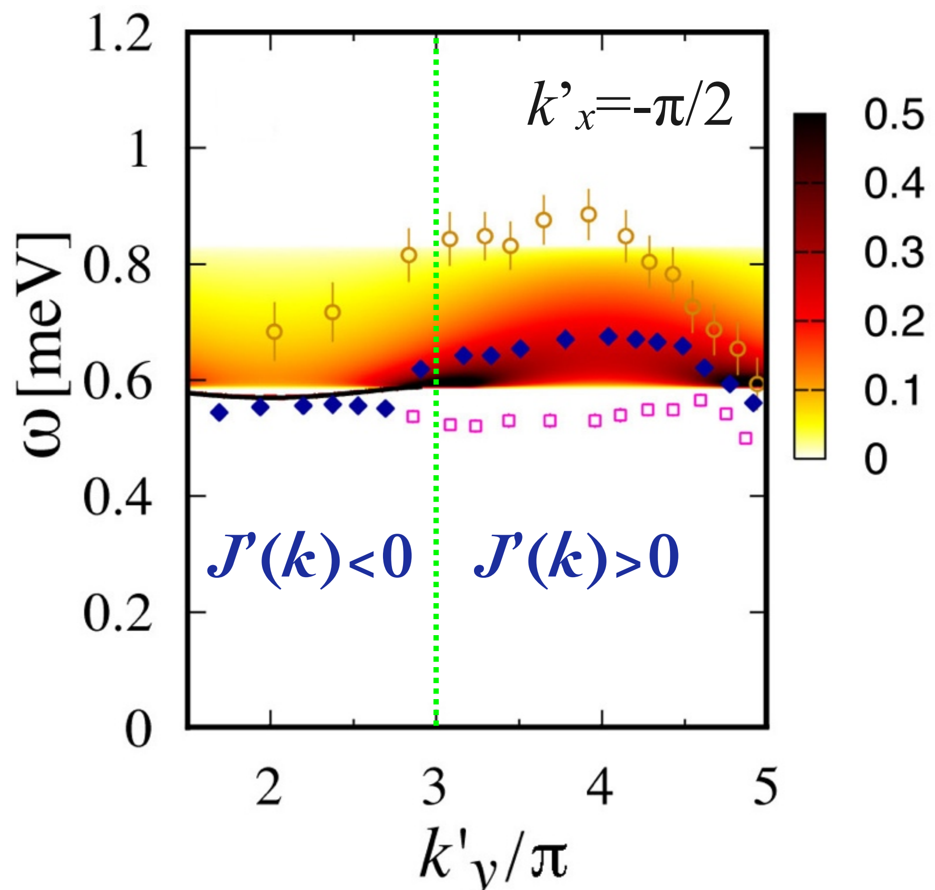

$$J'\left(k_x, k_y\right) = 4J'\cos\left(\frac{k'_x}{2}\right)\cos\left(\frac{k'_y}{2}\right).$$

Main peak(◆), upper edge(○) and lower edge(□) estimated experimentally by Coldea, *et al.*[1].

Dispersion Relation along k'_y

At k'_x=-π/2, the sign of $J'(\boldsymbol{k})$ changes at k'_y=3π. No fitting parameter

For k'_y<3π [$J'(\boldsymbol{k})$<0], a bound state is formed below the continuum.

For k'_y>3π [$J'(\boldsymbol{k})$>0], the peak is broadened in the continuum.

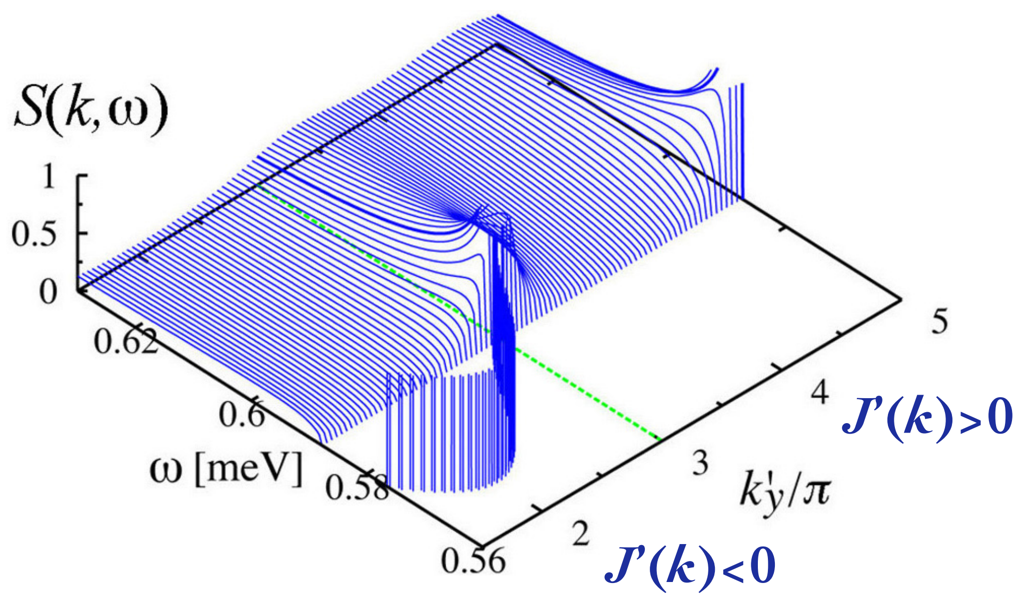

$S(k,\omega)$ at k'_x=-π/2 near the lower edge of the continuum by the present method.

$$J'(k_x,k_y) = 4J'\cos\left(\frac{k'_x}{2}\right)\cos\left(\frac{k'_y}{2}\right).$$

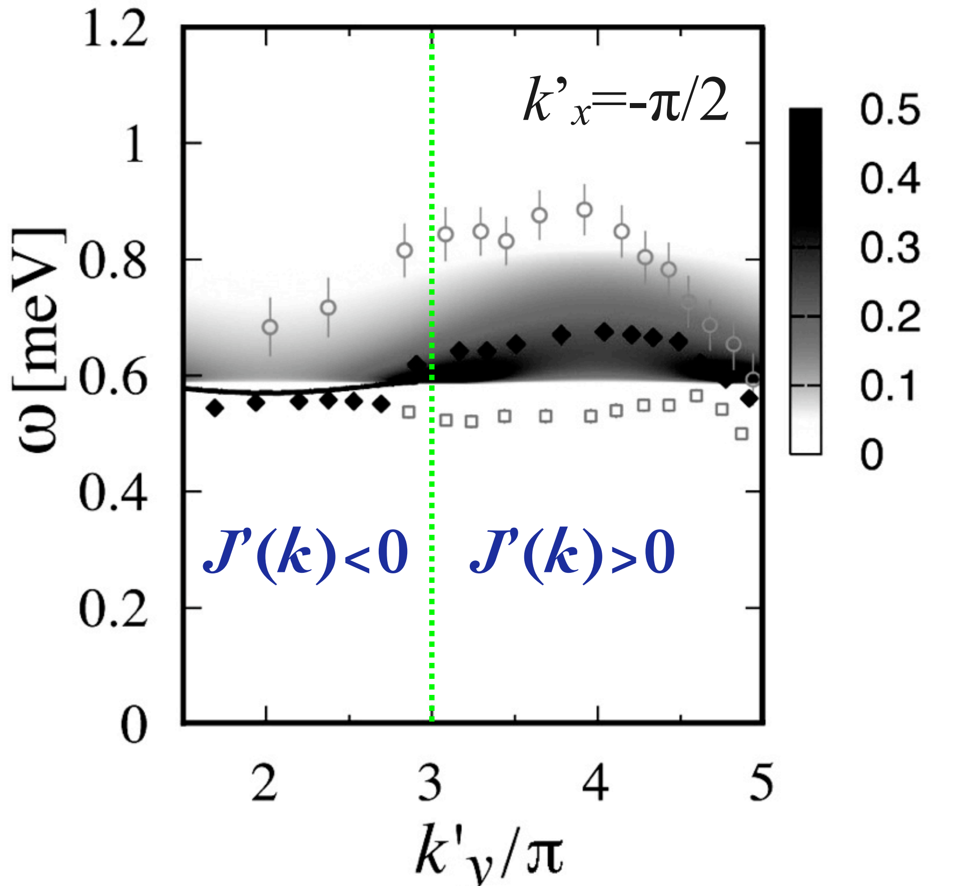

Main peak(◆), upper edge(○) and lower edge(□) estimated experimentally by Coldea, *et al.*[1].

Dispersion Relation along k'_y

At $k'_x=-\pi/2$, the sign of $J'(\boldsymbol{k})$ changes at $k'_y=3\pi$. No fitting parameter

For $k'_y<3\pi$ [$J'(\boldsymbol{k})<0$], a bound state is formed below the continuum.

For $k'_y>3\pi$ [$J'(\boldsymbol{k})>0$], the peak is broadened in the continuum.

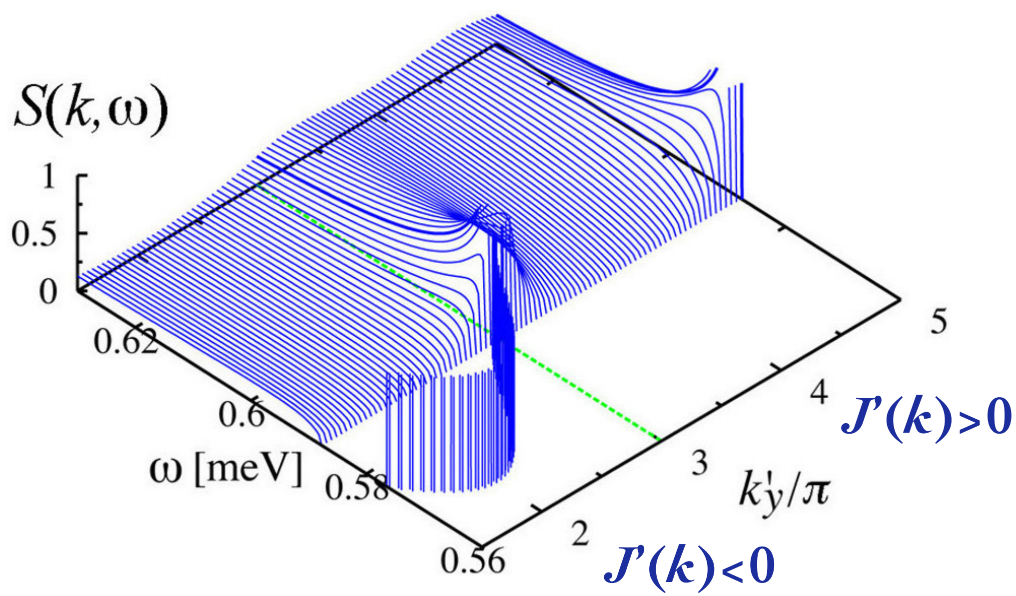

$S(k,\omega)$ at $k'_x=-\pi/2$ near the lower edge of the continuum by the present method.

$$J'\left(k_x,k_y\right) = 4J'\cos\left(\frac{k'_x}{2}\right)\cos\left(\frac{k'_y}{2}\right).$$

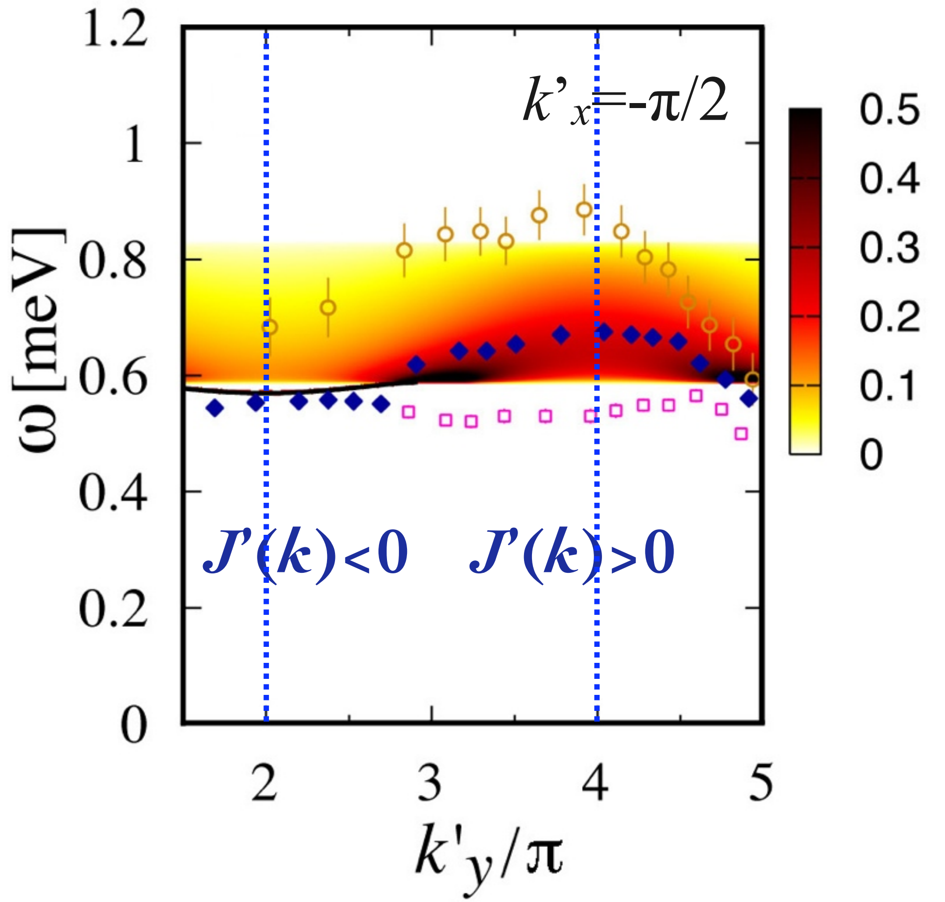

Main peak(◆), upper edge(○) and lower edge(□) estimated experimentally by Coldea, *et al.*[1].

Bound State and Broad Peak

For $J'(\boldsymbol{k})<0$, $S(\boldsymbol{k},\omega)$ has a sharp peak of the bound state. No fitting parameter

For $J'(\boldsymbol{k})>0$, $S(\boldsymbol{k},\omega)$ has a broad peak in the continuum.

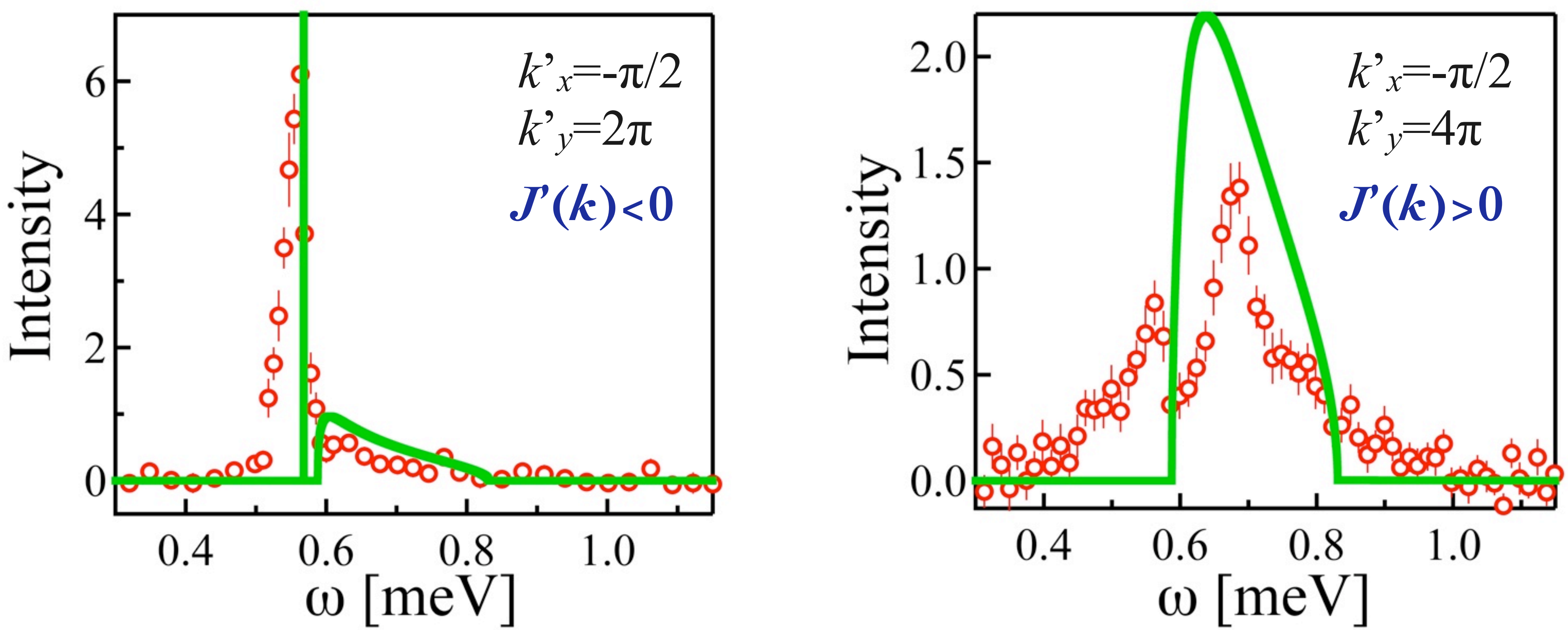

— : Present result (2-spinon)

o : Experimental result of Cs_2CuCl_4 by Coldea, *et al.*[1]

Bound State and Broad Peak

For $J'(\boldsymbol{k})<0$, $S(\boldsymbol{k},\omega)$ has a sharp peak of the bound state. No fitting parameter
For $J'(\boldsymbol{k})>0$, $S(\boldsymbol{k},\omega)$ has a broad peak in the continuum.

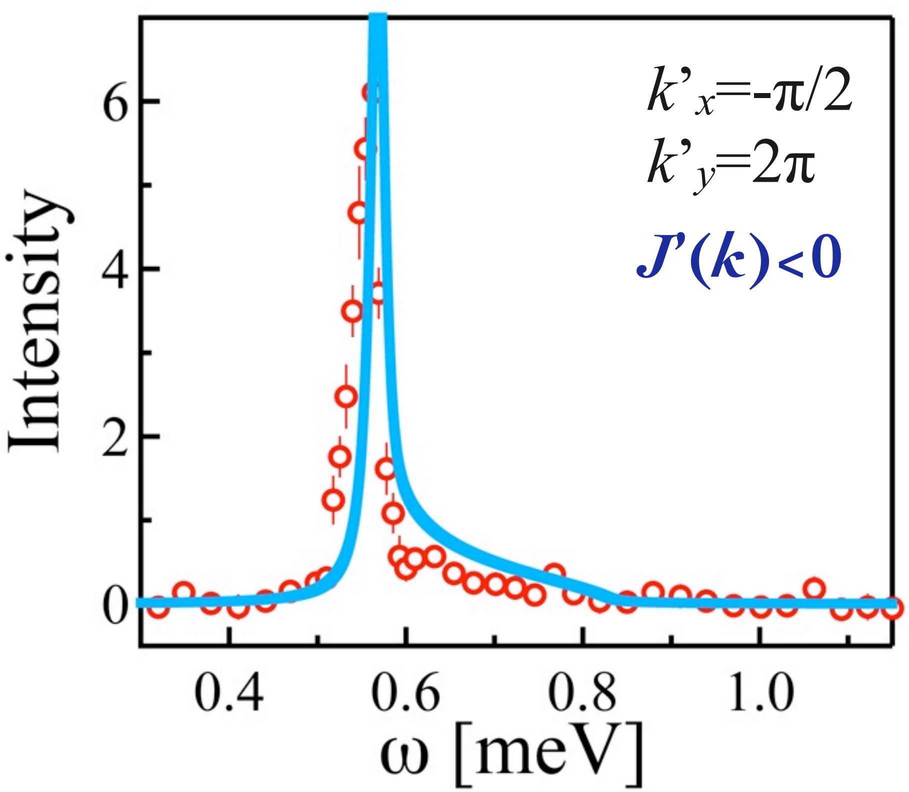

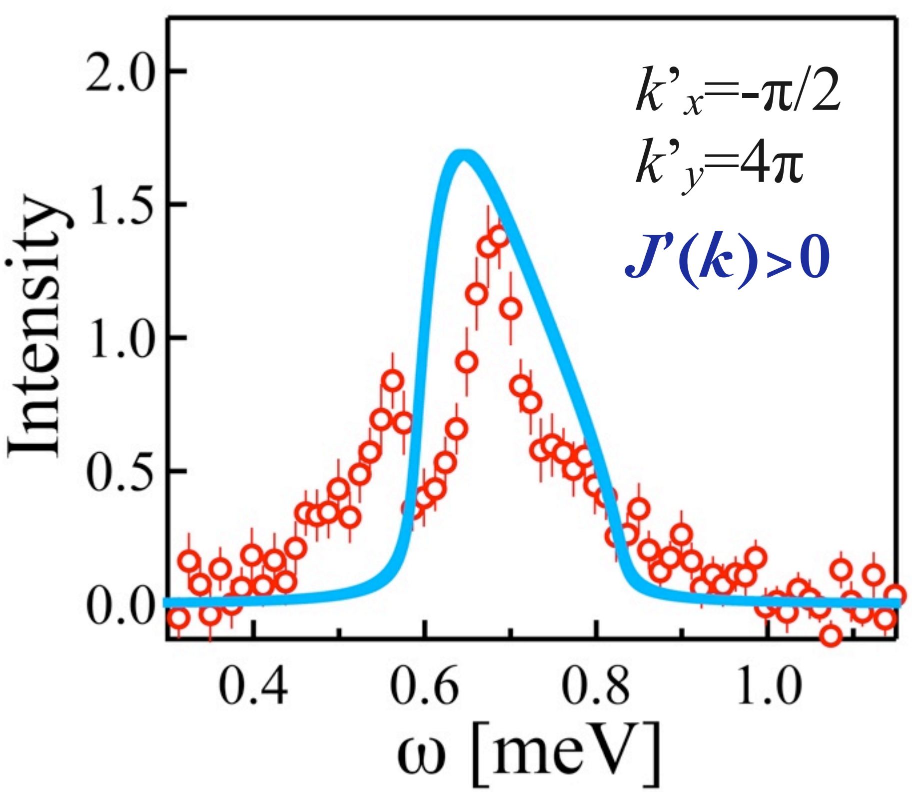

— : Present result (2-spinon) broadened by experimental resolution

o : Experimental result of Cs_2CuCl_4 by Coldea, *et al.*[1] (ΔE=0.019 meV)

Bound State and Broad Peak

For $J'(\boldsymbol{k})<0$, $S(\boldsymbol{k},\omega)$ has a sharp peak of the bound state. No fitting parameter

For $J'(\boldsymbol{k})>0$, $S(\boldsymbol{k},\omega)$ has a broad peak in the continuum.

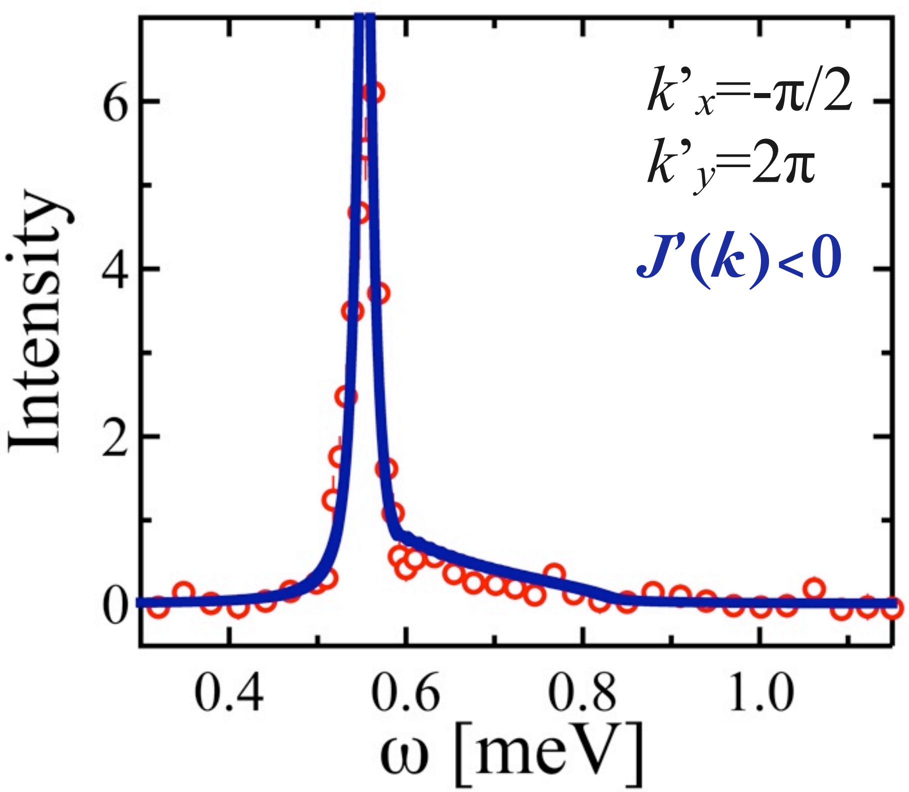

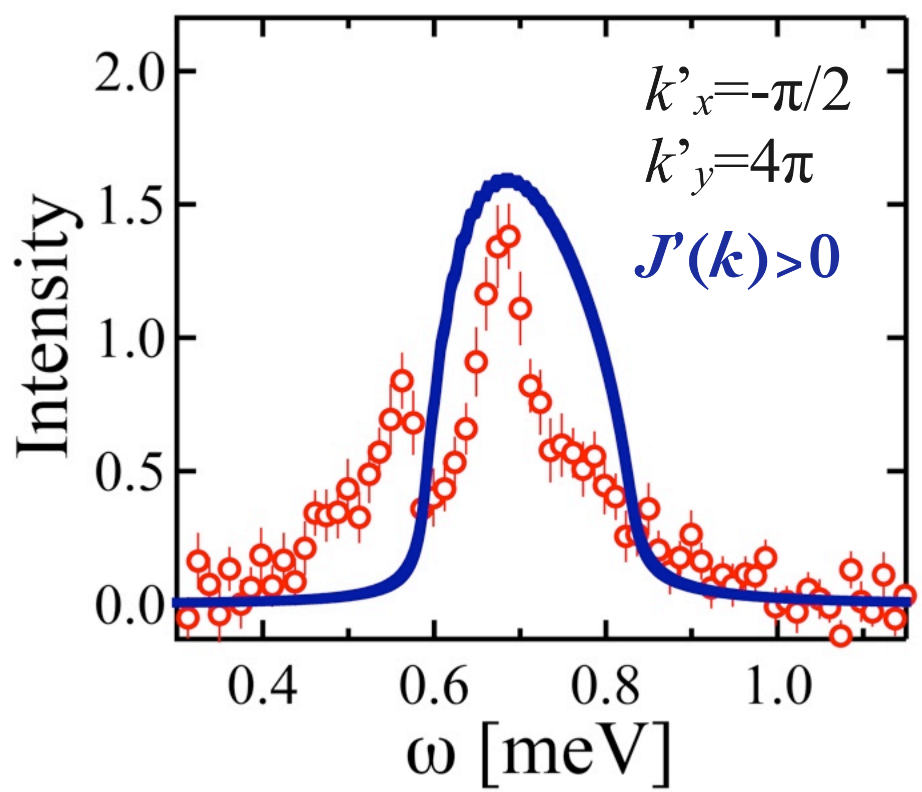

— : Present result (2- & 4-spinon, L_x=288) broadened by experimental resolution

o : Experimental result of Cs_2CuCl_4 by Coldea, *et al.*[1] (ΔE=0.019 meV)

Summary ~ Features in $S(k,\omega)$ ~

Three distinctive features of dynamical structure factor $S(\boldsymbol{k},\omega)$ are obtained depending on the momentum, which is classified by the sign of $J'(\boldsymbol{k})$.

$J'(\boldsymbol{k}) = 0$: The interchain interactions effectively vanish.
Spinons of the Heisenberg chain persist at these momenta.

$J'(\boldsymbol{k}) < 0$: Bound states of spinons appear below the continuum, where a spinon pair moves coherently like a magnon.
This bound state does not require ordered ground states.

$J'(\boldsymbol{k}) > 0$: Spectral weight shifts upwards.
The peak is broadened in the continuum.
Anti-bound state is observed above 2-spinon continuum.

In the present approach, power-law behaviors appear only at $J'(k_x,k_y)=0$.
The exponent $\eta=1$ (1D Heisenberg chain).

Summary ~ Comparison with Experiments ~

Unusual experimental features in Cs_2CuCl_4 have been consistently explained by the present approach basically without fitting parameter.

- Asymmetry of the dispersion relation :
  - Bound state below the continuum for $J'(\boldsymbol{k})<0$.
  - Broad peak in the continuum for $J'(\boldsymbol{k})>0$.

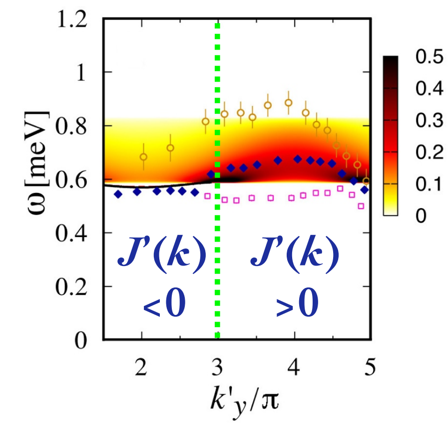

- Momentum dependence of line shape :

  Bound states are actually observed experimentally for $J'(\boldsymbol{k})<0$ as a sharp peak.

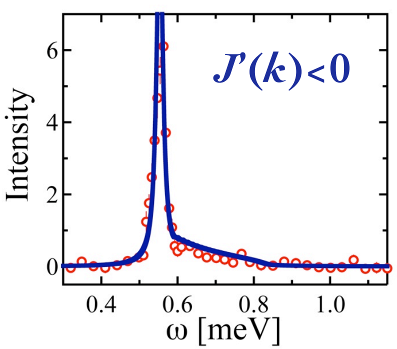

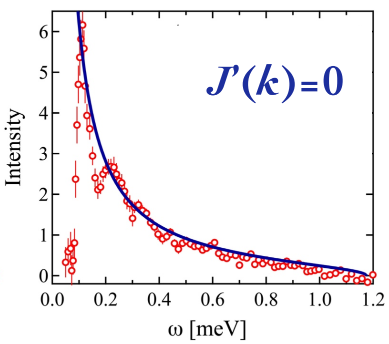

- Large tail at $k_x=\pi$:

  $S(\boldsymbol{k},\omega)$ at $J'(\boldsymbol{k})=0 \xrightarrow{\text{present approximation}} S_{1D}(k_x,\omega)$ (1D Heisenberg chain).
  Interpretation : descendants of 1D spinons strongly persist at $J'(\boldsymbol{k})=0$.